

AD-A245 323



2

NAVAL POSTGRADUATE SCHOOL Monterey, California



DTIC
ELECTE
JAN 31 1992
S B D

THESIS

ELECTROMAGNETIC SCATTERING FROM ROUGH
SURFACES USING THE ON-SURFACE
RADIATION BOUNDARY CONDITION (OSRC) METHOD

by

Spyridon G. Konidakis

December 1990

Thesis Advisor: Ramakrishna Janaswamy
Thesis Co-Advisor: R. Clark Robertson

Approved for public release; distribution is unlimited

92-02236



UNCLASSIFIED

SECURITY CLASSIFICATION OF THIS PAGE

REPORT DOCUMENTATION PAGE				Form Approved OMB No. 0704-0188	
1a. REPORT SECURITY CLASSIFICATION UNCLASSIFIED		1b. RESTRICTIVE MARKINGS			
2a. SECURITY CLASSIFICATION AUTHORITY		3. DISTRIBUTION / AVAILABILITY OF REPORT Approved for public release; distribution is unlimited			
2b. DECLASSIFICATION / DOWNGRADING SCHEDULE					
4. PERFORMING ORGANIZATION REPORT NUMBER(S)		5. MONITORING ORGANIZATION REPORT NUMBER(S)			
6a. NAME OF PERFORMING ORGANIZATION Naval Postgraduate School		6b. OFFICE SYMBOL (If applicable) EC	7a. NAME OF MONITORING ORGANIZATION Naval Postgraduate School		
6c. ADDRESS (City, State, and ZIP Code) Monterey, CA 93943-5000		7b. ADDRESS (City, State, and ZIP Code) Monterey, CA 93943-5000			
8a. NAME OF FUNDING / SPONSORING ORGANIZATION		8b. OFFICE SYMBOL (If applicable)	9. PROCUREMENT INSTRUMENT IDENTIFICATION NUMBER		
8c. ADDRESS (City, State, and ZIP Code)		10. SOURCE OF FUNDING NUMBERS			
		PROGRAM ELEMENT NO.	PROJECT NO.	TASK NO.	WORK UNIT ACCESSION NO.
11. TITLE (Include Security Classification) ELECTROMAGNETIC SCATTERING FROM ROUGH SURFACES USING THE ON-SURFACE RADIATION BOUNDARY CONDITION (OSRC) METHOD					
12. PERSONAL AUTHOR(S) KONIDARIS, Spyridon G.					
13a. TYPE OF REPORT Master's Thesis		13b. TIME COVERED FROM _____ TO _____	14. DATE OF REPORT (Year, Month, Day) 1990 December		15. PAGE COUNT 89
16. SUPPLEMENTARY NOTATION The views expressed in this thesis are those of the author and do not reflect the official policy or position of the Department of Defense or the US Government.					
17. COSATI CODES			18. SUBJECT TERMS (Continue on reverse if necessary and identify by block number)		
FIELD	GROUP	SUB-GROUP	electromagnetic scattering; period surfaces		
19. ABSTRACT (Continue on reverse if necessary and identify by block number) Electromagnetic scattering from rough surfaces is of prime importance in the engineering field since it affects communications, radar, remote sensing, acoustics, etc. The actual problem of scattering from rough surfaces is complicated and involves three dimensional scattering from either lossy or dielectric, electrically large surfaces. Integral equations are widely utilized to solve this kind of problem but this solution to the problem is generally computationally intensive. In the On-Surface Radiation Boundary Condition (OSRC) method, a higher order radiation condition is imposed directly on the surface of the scatterer. This reduces the integral equation for the scattered field to a line integral which can be easily evaluated numerically. In this thesis, the OSRC method is used to formulate the problem of					
20. DISTRIBUTION / AVAILABILITY OF ABSTRACT <input checked="" type="checkbox"/> UNCLASSIFIED/UNLIMITED <input type="checkbox"/> SAME AS RPT. <input type="checkbox"/> DTIC USERS			21. ABSTRACT SECURITY CLASSIFICATION UNCLASSIFIED		
22a. NAME OF RESPONSIBLE INDIVIDUAL JANASWAMY, Ramakrishna			22b. TELEPHONE (Include Area Code) 408-646-3217		22c. OFFICE SYMBOL EC/Js

DD Form 1473, JUN 86

Previous editions are obsolete.

SECURITY CLASSIFICATION OF THIS PAGE

S/N 0102-LF-014-6603

UNCLASSIFIED

19. cont.

scattering from periodic rough, n -dimensional surfaces illuminated by a transverse magnetic, plane electromagnetic wave. Three geometric surfaces are considered. A comparison is made between the present formulation, the exact solution, and the physical optics approximation.

Approved for public release; distribution is unlimited

Electromagnetic Scattering from Rough Surfaces Using
the On-Surface Radiation Boundary Condition (OSRC) Method

by

Spyridon G. Konidaris
Lieutenant J.G., Hellenic Navy
B.S., Hellenic Naval Academy, 1982

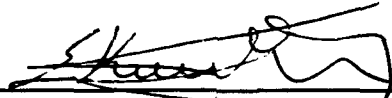
Submitted in partial fulfillment of the
requirements of degree of

MASTER OF SCIENCE IN ELECTRICAL ENGINEERING

from the

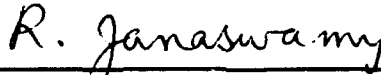
NAVAL POSTGRADUATE SCHOOL
December 1990

Author:

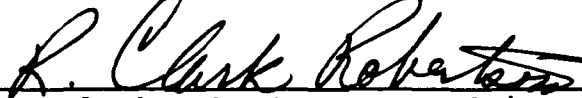


Spyridon G. Konidaris

Approved by:



Ramakrishna Janaswamy, Thesis Advisor



R. Clark Robertson, Co-Advisor



Michael A. Morgan, Chairman
Department of Electrical and Computer Engineering



Accession For	
NTIS GRA&I	<input checked="" type="checkbox"/>
DTIC TAB	<input type="checkbox"/>
Unannounced	<input type="checkbox"/>
Justification	
By	
Distribution/	
Availability Codes	
Dist	Avail and/or Special
A-1	

ABSTRACT

Electromagnetic scattering from rough surfaces is of prime importance in the engineering field since it affects communications, radar, remote sensing, acoustics, etc. The actual problem of scattering from rough surfaces is complicated and involves three dimensional scattering from either lossy or dielectric, electrically large surfaces. Integral equations are widely utilized to solve this kind of problem but this solution to the problem is generally computationally intensive.

In the On-Surface Radiation Boundary Condition (OSRC) method, a higher order radiation condition is imposed directly on the surface of the scatterer. This reduces the integral equation for the scattered field to a line integral which can be easily evaluated numerically.

In this thesis, the OSRC method is used to formulate the problem of scattering from periodic rough, two-dimensional surfaces illuminated by a transverse magnetic, plane electromagnetic wave. Three geometric surfaces are considered. A comparison is made between the present formulation the exact solution, and the physical optics approximation.

TABLE OF CONTENTS

I.	INTRODUCTION.....	1
A.	HISTORY.....	1
B.	ON-SURFACE RADIATION CONDITION (OSRC) METHOD.....	1
C.	STATEMENT OF THE PROBLEM.....	2
II.	FORMULATION.....	4
A.	NOMENCLATURE.....	4
B.	GENERAL THEORY.....	5
C.	SURFACE CURRENT AND ECHO WIDTH.....	13
III.	THIN CONDUCTING STRIP.....	15
A.	SURFACE CURRENT.....	15
B.	FAR-FIELD ECHO WIDTH.....	18
IV.	SCATTERING FROM TRIANGULAR AND SINUSOIDAL PERFECTLY CONDUCTING SURFACE.....	19
A.	TRIANGULAR CASE.....	19
B.	SINUSOIDAL CASE.....	21
V.	NUMERICAL RESULTS.....	25
A.	SURFACE CURRENT COMPARISONS.....	26
B.	ECHO WIDTH COMPUTATIONS - COMPARISONS.....	28
VI.	CONCLUSIONS.....	45
A.	SUMMARY.....	45
B.	RECOMMENDATIONS.....	46
APPENDIX A	MATHEMATIC DERIVATIONS.....	47
APPENDIX B	EVALUATION OF INTEGRALS.....	50
APPENDIX C	PROGRAMS.....	54
REFERENCES.....		81
INITIAL DISTRIBUTION LIST.....		82

ACKNOWLEDGEMENTS

I would like to express my thanks to Professor Ramakrishna Janaswamy, my thesis advisor, for his experienced guidance in this thesis.

This thesis is dedicated to my wife, Evangelia, for her continuing and encouraging love, understanding, and patience throughout my stay at the Naval Postgraduate School; to my sons, George and Michael, who have brought so much happiness into my life, and to my beloved parents.

Finally, I wish to thank the Hellenic Navy, for providing this opportunity, and the Greek taxpayers for having paid the expenses for my course of study at NPS.

I. INTRODUCTION

A. HISTORY

The problem of scattering from periodic rough surfaces has aroused the interest of physicists and engineers for the last 70 years and has become of special interest in recent years, particularly in connection with the propagation of radio waves at frequencies above 30 MHz. The problem of scattering from rough surfaces arises, among others, in line-of-sight as well as mobile radio communication, radar, sea scattering, remote sensing, tropospheric propagation, radio astronomy, and acoustics.

Mathematically, the problem of the scattering of waves by a rough surface is difficult to formulate and even more difficult to obtain numerical results.

B. ON-SURFACE RADIATION CONDITION (OSRC) METHOD

Recently, a new formulation of electromagnetic scattering has been introduced [Ref. 1]. This formulation of electromagnetic wave scattering by convex, two-dimensional conducting bodies, the On-Surface Radiation Condition (OSRC) approach, is based upon an expansion of the radiation condition applied directly on the surface of a scatterer. According to the OSRC approach, the application of a suitable radiation condition directly on the conducting scattering surface can lead to substantial simplification of the frequency-domain integral equation for the scattered field.

For the transverse magnetic (TM) case, the integrand is known explicitly. For the transverse electric (TE) case, the integrand can be constructed by solving an ordinary differential equation around the scatterer surface contour. Implicit in the OSRC formulation is the fact that only outgoing waves are assumed to exist on the surface of the scatterer. Thus, the method will have serious drawbacks in cases where the latter condition is not met.

C. STATEMENT OF THE PROBLEM

In this thesis we apply the OSRC technique to scattering by a periodic rough surface. We consider a plane electromagnetic wave illuminating a two-dimensional, perfectly conducting periodic rough surface for the transverse magnetic (TM) polarization case (magnetic field parallel to the propagation plane or electric field parallel to the surface ridges as in Figure 1).

The analysis of this problem includes the calculation of the induced electric current as well as the echo width of the scattering surfaces. Both of these quantities are calculated in Chapter II.

In Chapter III, we calculate the current distribution and the echo width of a planar thin conducting strip, while in Chapter IV we calculate the same two quantities for a sinusoidal scattering surface and the surface current distribution on a scatterer of triangular shape.

The numerical results of the current distributions as well as the echo width of the planar strip and the sinusoidal surface are presented in Chapter V. Comparisons of these results with results from the physical optics approximation and with the exact solution (method of moments), are also presented in this chapter.

In Chapter VI, conclusions and recommendations are presented. Some mathematical derivations and the computer codes developed to evaluate and test our results are listed in the appendices.

II. FORMULATION

In this thesis we apply the OSRC technique to scattering by a rough surface. In this chapter we will formulate the problem and calculate both the surface current and the far-field echo width of a periodic rough, perfectly conducting surface.

A. NOMENCLATURE

We will consider a plane electromagnetic wave illuminating a two-dimensional, perfectly conducting, rough surface for the transverse magnetic (TM) polarization case (Figure 1). The width of the rough surface is considered finite and edge effects are ignored.

We shall use Cartesian coordinates x, y, z with origin 0 and unit vectors $\hat{x}, \hat{y}, \hat{z}$. The two dimensional rough surface is specified by the function $z = f(x)$ where the mean level of this surface is the plane $z = 0$.

All quantities, except angles, associated with the incident field will be denoted by the superscript i and those associated with the scattered field by the superscript s . Thus, the incident field is \vec{E}^i and the scattered field \vec{E}^s . The medium above the surface is assumed to be free space. We shall assume \vec{E}^i to be linearly polarized. This implies that we need only the scalar value U^s of the vector \vec{E}^i .

B. GENERAL THEORY

For TM polarization, the incident electric field \vec{E}^i propagating perpendicular to the x - z plane at an angle θ_0 with respect to the $+z$ axis, as shown in Figure 1, is given [Ref. 2]

$$\vec{E}^i = U^i e^{j\omega t} \hat{y} \quad (2.1)$$

where U^i is the magnitude of the incident electric field

$$U^i = e^{-jk_0(x \sin \theta_0 - z \cos \theta_0)} \quad (2.2)$$

k_0 is the wavenumber of the free space defined as

$$k_0 = \frac{2\pi}{\lambda_0} = \frac{2\pi f_0}{c} \quad (2.3)$$

and harmonic time dependence is assumed. The quantity λ_0 is the free space wavelength associated with the incident electromagnetic wave of frequency f_0 , c is the speed of light in free space, and $\omega = 2\pi f_0$ is the radian frequency of the incident wave.

The scattered electric field \vec{E}^s is [Ref. 2]

$$\vec{E}^s = U^s e^{j\omega t} \hat{y} \quad (2.4)$$

where U^s is given, in the far-field, by [Ref. 1]

$$U^s = \frac{e^{-j(k_0 r - \frac{\pi}{4})}}{[8k_0 \pi r]^{\frac{1}{2}}} \int_{c'} \left[\frac{\partial U^s}{\partial n'} + jk_0 \cos \delta U^i \right] e^{jk_0 R \cos \delta} ds' \quad (2.5)$$

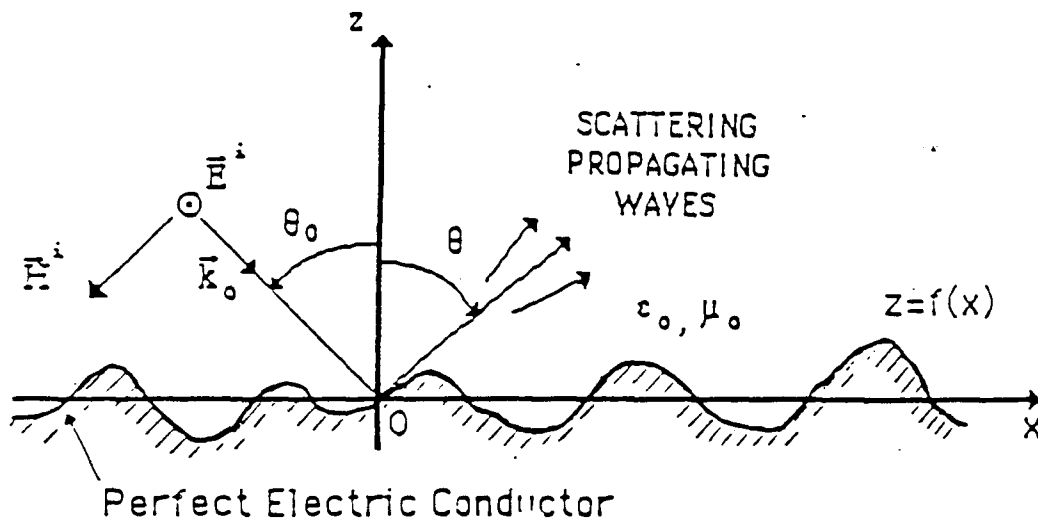


Figure 1 Scattering geometry for a TM polarized incident plane wave.

where C represents the contour of the surface, \hat{n}' is the unit vector normal to the curve C at point $P(x', z')$, as shown in Figure 2, and $\partial / \partial n'$ denotes an outward normal derivative on C . Note the integration in Equation (2.5) is with respect to the arc length, s' , corresponding to the point $P(x', z')$ at distance R from the origin, and that r is the distance of the observation point from the origin. The unit vector \hat{f} in the direction of the observation point is

$$\hat{f} = \sin\theta \cdot \hat{x} + \cos\theta \cdot \hat{z} \quad (2.6)$$

where θ is the scattering angle, measured in opposite sense to the incidence angle θ_0 .

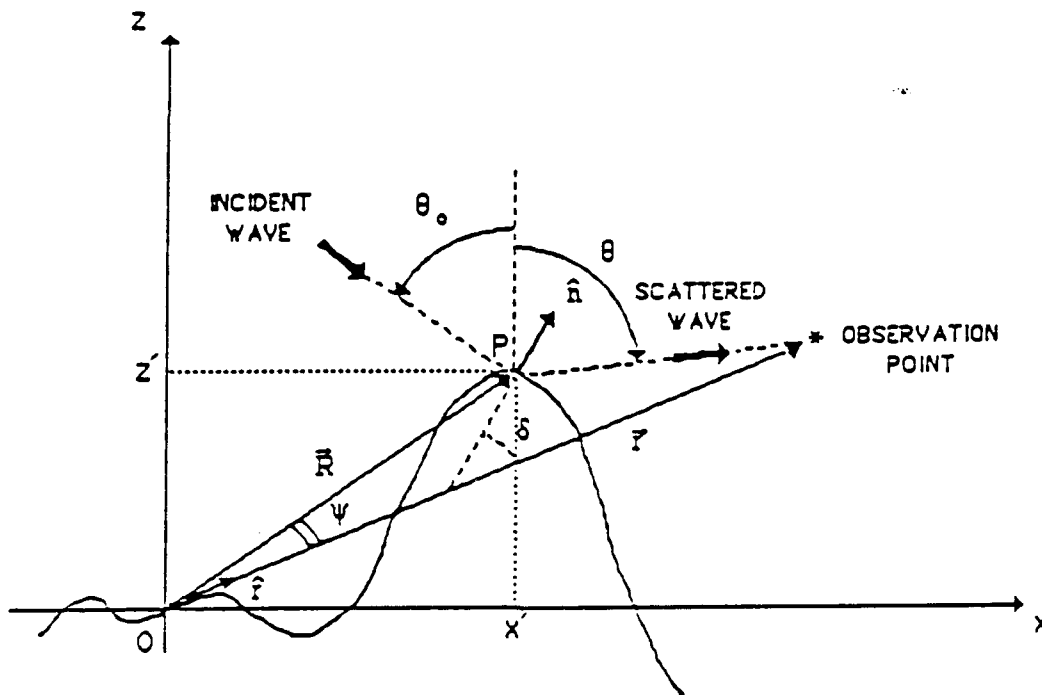


Figure 2 Notation for various vectors and angles.

In Equation (2.5), the terms $\cos\delta$ and $R\cos\psi$ are given by

$$\cos\delta = \hat{p} \cdot \hat{n}' \quad (2.7)$$

$$R\cos\psi = \vec{R} \cdot \hat{p} \quad (2.8)$$

where

$$\vec{R} = x'\hat{x} + z'\hat{z} \quad (2.9)$$

The unknown quantity $\partial U^s / \partial n'$ can be expressed in terms of the incident field using the second order radiation boundary condition. It is given by [Ref. 1]

$$\frac{\partial U^s}{\partial n'} = \left[\frac{\zeta(x')}{2} + jk_0 + \frac{\zeta^2(x')}{8[-jk_0 - \zeta(x')]} \right] U^i + \frac{1}{2[-jk_0 - \zeta(x')]} \frac{\partial^2 U^i}{\partial s'^2} \quad (2.10)$$

where $\zeta(x')$ is the curvature of the two dimensional scattering surface at point $P(x', z')$ and $\partial^2 / \partial s'^2$ is the second derivative with respect to the arc length of C .

The curvature $\zeta(x)$ of the curve C that is defined by an equation of the type $z = f(x)$ is given by [Ref. 3]

$$\zeta(x) = \frac{\left| \frac{d^2 z}{dx^2} \right|}{\left[1 + \left(\frac{dz}{dx} \right)^2 \right]^{\frac{3}{2}}} \quad (2.11)$$

while the quantity $\partial^2 U^i / \partial s'^2$ is shown in Appendix A to be

$$\begin{aligned} \frac{\partial^2 U^i}{\partial s'^2} = U^i & \left[\frac{-k_0^2 \sin^2 \theta_0 + k_0^2 \frac{dz}{dx} \cos \theta_0 \left(2 \sin \theta_0 - \frac{dz}{dx} \cos \theta_0 \right) + jk_0 \frac{d^2 z}{dx^2} \cos \theta_0}{1 + \left(\frac{dz}{dx} \right)^2} \right. \\ & \left. + jk_0 \frac{(\sin \theta_0 - \frac{dz}{dx} \cos \theta_0) \frac{dz}{dx} \frac{d^2 z}{dx^2}}{\left[1 + \left(\frac{dz}{dx} \right)^2 \right]^2} \right] \quad (2.12) \end{aligned}$$

By substituting Equations (2.11), (2.12), into Equation (2.10) and carrying out some manipulation, we get

$$\begin{aligned}
\frac{\partial U^s}{\partial n'} = & U^i \left(\frac{\left| \frac{d^2 z}{dx^2} \right|}{2 \left[1 + \left(\frac{dz}{dx} \right)^2 \right]^{\frac{3}{2}}} \left[1 - \frac{\left| \frac{d^2 z}{dx^2} \right|}{4 \left(jk_0 \left[1 + \left(\frac{dz}{dx} \right)^2 \right]^{\frac{3}{2}} + \left| \frac{d^2 z}{dx^2} \right| \right)} \right] + jk_0 \right. \\
& + \frac{\left[1 + \left(\frac{dz}{dx} \right)^2 \right]^{\frac{1}{2}}}{2 \left(jk_0 \left[1 + \left(\frac{dz}{dx} \right)^2 \right]^{\frac{3}{2}} + \left| \frac{d^2 z}{dx^2} \right| \right)} \left[k_0^2 \left(\sin^2 \theta_0 + \cos \theta_0 \frac{dz}{dx} \left(2 \sin \theta_0 - \frac{dz}{dx} \cos \theta_0 \right) \right) \right. \\
& \left. \left. + jk_0 \frac{d^2 z}{dx^2} \left(\cos \theta_0 + \frac{\left(\sin \theta_0 - \frac{dz}{dx} \cos \theta_0 \right) \frac{dz}{dx}}{1 + \left(\frac{dz}{dx} \right)^2} \right) \right] \right] \quad (2.13)
\end{aligned}$$

The quantity $\partial U^s / \partial n'$ is expressed in terms of U^i and hence is completely known at all points on the rough surface.

The unit vector \hat{n}' , normal to the curve C at point $P(x', z')$, is given by [Ref. 3]

$$\hat{n} = \pm \left(- \frac{\frac{dz}{dx}}{\left[1 + \left(\frac{dz}{dx} \right)^2 \right]^{\frac{1}{2}}} \hat{x} + \frac{1}{\left[1 + \left(\frac{dz}{dx} \right)^2 \right]^{\frac{1}{2}}} \hat{z} \right) \quad (2.14)$$

where the upper sign corresponds to the outward normal and the lower sign to the inward normal.

The formula for the partial derivative of the incident electric field with respect to the outward normal vector, which we will use later, is given by

$$\frac{\partial U^i}{\partial n'} = (\nabla U^i) \cdot \hat{n}' = jkU^i \frac{\frac{dz}{dx} \sin\theta_0 + \cos\theta_0}{\left[1 + \left(\frac{dz}{dx}\right)^2\right]^{\frac{1}{2}}} \quad (2.15)$$

Substituting Equations (2.6) and (2.14) into Equation (2.7), we get

$$\cos\delta = \hat{p} \cdot \hat{n} = \frac{-\frac{dz}{dx} \sin\theta + \cos\theta}{\left[1 + \left(\frac{dz}{dx}\right)^2\right]^{\frac{1}{2}}} \quad (2.16)$$

Likewise substituting Equations (2.9) and (2.6) into Equation (2.8), we get

$$k_0 R \cos\psi = k_0 (\vec{R} \cdot \hat{p}) = k_0 (x \sin\theta + z \cos\theta) \quad (2.17)$$

We will normalize all dimensions to the free space wavenumber k_0 . Accordingly, we let

$$\rho = k_0 x, \quad \tau = k_0 z \quad (2.18)$$

so that

$$dx = \frac{1}{k_0} d\rho, \quad dz = \frac{1}{k_0} d\tau \quad (2.19)$$

and

$$\frac{dz}{dx} = \frac{d\tau}{d\rho}, \quad \frac{d^2 z}{dx^2} = k_0 \frac{d^2 \tau}{d\rho^2} \quad (2.20)$$

Combining Equations (2.18), (2.19) and (2.20) with Equations (2.2), (2.16), (2.17) and (2.13), we express all quantities in terms of the normalized variables ρ, τ as

$$U^i = e^{-j(\rho \sin \theta_0 - \tau \cos \theta_0)} \quad (2.21)$$

$$\cos \delta = \frac{-\frac{d\tau}{d\rho} \sin \theta + \cos \theta}{\left[1 + \left(\frac{d\tau}{d\rho}\right)^2\right]^{\frac{1}{2}}} \quad (2.22)$$

$$k_0 R \cos \psi = \rho \sin \theta + \tau \cos \theta \quad (2.23)$$

$$\begin{aligned} \frac{\partial U^s}{\partial n'} = & k_0 U^i \left(\frac{\left| \frac{d^2 \tau}{d\rho^2} \right|}{2 \left[1 + \left(\frac{d\tau}{d\rho} \right)^2 \right]^{\frac{3}{2}}} \left[1 - \frac{\left| \frac{d^2 \tau}{d\rho^2} \right|}{4 \left(j \left[1 + \left(\frac{d\tau}{d\rho} \right)^2 \right]^{\frac{3}{2}} + \left| \frac{d^2 \tau}{d\rho^2} \right| \right)} \right] + j \right. \\ & + \frac{\left[1 + \left(\frac{d\tau}{d\rho} \right)^2 \right]^{\frac{1}{2}}}{2 \left(j \left[1 + \left(\frac{d\tau}{d\rho} \right)^2 \right]^{\frac{3}{2}} + \left| \frac{d^2 \tau}{d\rho^2} \right| \right)} \left[\sin^2 \theta_0 + \frac{d\tau}{d\rho} \cos \theta_0 \left(2 \sin \theta_0 - \frac{d\tau}{d\rho} \cos \theta_0 \right) \right. \\ & \left. \left. + j \frac{d^2 \tau}{d\rho^2} \left(\cos \theta_0 + \frac{\left(\sin \theta_0 - \frac{d\tau}{d\rho} \cos \theta_0 \right) \frac{d\tau}{d\rho}}{1 + \left(\frac{d\tau}{d\rho} \right)^2} \right) \right] \right) \quad (2.24) \end{aligned}$$

The arc length s is related to the surface $z(x)$ by [Ref.

3]

$$s = \int_a^x \left[1 + \left(\frac{dz}{dx} \right)^2 \right]^{\frac{1}{2}} dx \quad (2.25)$$

so that the differential arc length ds' can be expressed in terms of the normalized coordinates as

$$ds' = \frac{1}{k_0} \left[1 + \left(\frac{d\tau}{d\rho} \right)^2 \right]^{\frac{1}{2}} d\rho' \quad (2.26)$$

Substituting Equation (2.26) in Equation (2.5), we get:

$$U^s = \frac{e^{-j(k_0 r - \frac{\pi}{4})}}{[8k_0 \pi r]^{\frac{1}{2}}} \int_c \left(\left[\frac{\partial U^s}{\partial n'} + jk_0 \cos \delta U^i \right] \frac{e^{jk_0 R \cos \psi}}{k_0} \left[1 + \left(\frac{d\tau}{d\rho} \right)^2 \right]^{\frac{1}{2}} \right) d\rho' \quad (2.27)$$

To organize our work better and to enable more efficient structural programming, we rewrite the above equation as

$$U^s = V(r) \cdot \int_c (F(\rho) \cdot Q(\rho)) d\rho \quad (2.28)$$

where

$$V(r) = \frac{e^{-j(k_0 r - \frac{\pi}{4})}}{[8k_0 \pi r]^{\frac{1}{2}}} \quad (2.29)$$

$$F(\rho) = \frac{\partial U^s}{\partial n'} + jk_0 \cos \delta U^i \quad (2.30)$$

$$Q(\rho) = \frac{e^{jk_0 R \cos \psi}}{k_0} \left[1 + \left(\frac{d\tau}{d\rho} \right)^2 \right]^{\frac{1}{2}} \quad (2.31)$$

and $\partial U^s / \partial n'$, $\cos \delta$, U^i and $k_0 R \cos \psi$ as given by Equations (2.24), (2.22), (2.21) and (2.23) respectively.

C. SURFACE CURRENT AND ECHO WIDTH

Two quantities needed to compare our results with those in the literature are the electric surface current induced on the scattering surface and the far field echo width of this surface. These quantities will be presented next.

Since $U^{Tot} = U^i + U^s$ and the total magnetic field is given by

$$\mathbf{H}^{Tot} = \bar{y} \frac{1}{j\omega\mu_0} \frac{\partial U^{Tot}}{\partial n} \quad (2.32)$$

the normalized electric current on the scattering surface, equal to the ratio of the total to the incident magnetic field, is

$$\frac{\mathbf{H}^{Tot}}{\mathbf{H}^i} = \frac{1}{j\omega\mu_0 \mathbf{H}^i} \left(\frac{\partial U^s}{\partial n} + \frac{\partial U^i}{\partial n} \right) \quad (2.33)$$

In the Equation (2.33) the only previously undefined term is the magnitude of the incident magnetic field, \mathbf{H}^i , which can be obtained in terms of the electric field using the Maxwell's equation [Ref. 4]

$$\mathbf{H}^i = -\frac{1}{j\omega\mu_0} (\nabla \times \mathbf{E}) = \frac{j}{\omega\mu_0} \left(-\frac{\partial U^i}{\partial z} \hat{x} + \frac{\partial U^i}{\partial x} \hat{z} \right) \quad (2.34)$$

For the case of a plane incident wave

$$H^i = |\vec{H}^i| = \frac{k_0}{\omega \mu_0} = \frac{1}{\eta_0} \quad (2.35)$$

where η_0 is the intrinsic impedance of the free space.

The normalized surface electric current is now given by

$$\frac{H^{tot}}{H^i} = \frac{1}{jk_0} \left(\frac{\partial U^s}{\partial n} + \frac{\partial U^i}{\partial n} \right) = -jU^i \left[\frac{1}{k_0 U^i} \left(\frac{\partial U^s}{\partial n} + \frac{\partial U^i}{\partial n} \right) \right] \quad (2.36)$$

The far-field echo width σ of the scattering surface is defined as [Ref. 2]

$$\sigma = \lim_{r \rightarrow \infty} \left(\frac{|\bar{U}^s|^2}{|\bar{U}^i|^2} 2\pi r \right) \quad (2.37)$$

Since all quantities have been previously defined, σ can be easily calculated.

III. THIN CONDUCTING STRIP

The mathematical derivations of the previous chapter are for an arbitrary rough surface. In this chapter we specialize to the case of TM scattering by a thin conducting strip. Because results for the induced current and echo width for a conducting strip are known by other means this will serve as a check to our formulation.

A. SURFACE CURRENT

For a thin planar perfectly conducting strip with the geometry of Figure 3, the surface is described by

$$z = ax \quad , \quad \tau = ap \tag{3.1}$$

where a is the slope of the surface.

Using the results of the previous chapter, the normalized surface electric current density on this surface is given by

$$\frac{H^{rot}}{H^i} = U^i \left[\left(1 - \frac{\sin^2\theta_0 + a\cos\theta_0(2\sin\theta_0 - a\cos\theta_0)}{2(1+a^2)} \right) + \frac{a\sin\theta_0 + \cos\theta_0}{[1+a^2]^{\frac{1}{2}}} \right] \tag{3.2}$$

Notice that the current distribution is known analytically. This is in contrast to other methods where differential or integral equations must be solved to obtain the current distribution.

Let us now derive a formula for the scattered echo width. According to Appendix B, we can express the integral in

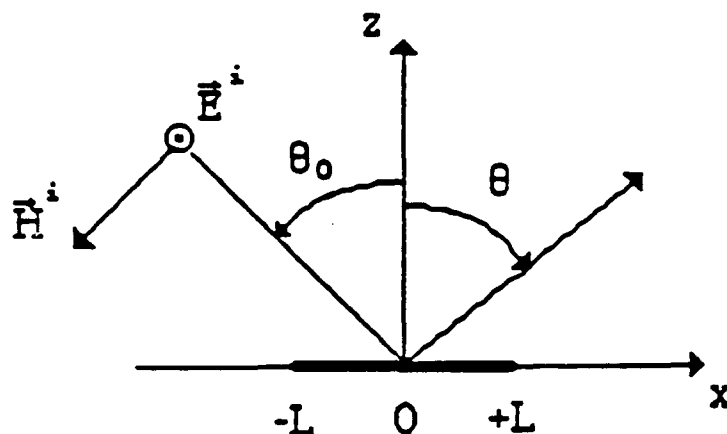


Figure 3 Planar, thin conducting strip profile, illuminated by a TM polarized, plane wave.

Equation (2.28) as

$$\int_c F(\rho) \cdot Q(\rho) d\rho = 2 \int_{\rho=-k_0L}^{\rho=+k_0L} \frac{\partial U^s}{\partial n} Q(\rho) d\rho \quad (3.3)$$

Equation (2.27) becomes

$$U^s = V(x) 2 \int_{\rho=-k_0L}^{\rho=+k_0L} \left(\frac{1}{k_0 U^i} \frac{\partial U^s}{\partial n} \right) U^i e^{jk_0 R \cos \psi} \left[1 + \left(\frac{d\tau}{d\rho} \right)^2 \right]^{\frac{1}{2}} d\rho \quad (3.4)$$

Note that no special consideration for the fields is given at the edges $x = \pm L$.

Other quantities needed to evaluate the integral are

$$U^i = e^{-j\rho(\sin\theta_0 - a\cos\theta_0)} \quad (3.5)$$

$$k_0 R \cos\psi = \rho(\sin\theta + a\cos\theta) \quad (3.6)$$

$$\frac{1}{k_0 U^i} \frac{\partial U^s}{\partial n} = j \left(1 - \frac{1}{2[1+a^2]} D \right) \quad (3.7)$$

where

$$D = \sin^2\theta_0 + a\cos\theta_0(2\sin\theta_0 - a\cos\theta_0) \quad (3.8)$$

Substituting the above equations into Equation (3.4), we get

$$U^s = V(r) 2j \left(1 - \frac{D}{2[1+a^2]} \right) [1+a^2]^{\frac{1}{2}} \int_{-k_0 L}^{+k_0 L} e^{jG\rho} d\rho \quad (3.9)$$

where

$$G = (\sin\theta - \sin\theta_0) + a(\cos\theta + \cos\theta_0) \quad (3.10)$$

The integral in Equation (3.9) can be evaluated in closed form. Carrying out the integration and substituting for $V(r)$, we get

$$U^s = 4j \left[\frac{1+a^2}{8k_0\pi r} \right]^{\frac{1}{2}} \left(1 - \frac{D}{2[1+a^2]} \right) k_0 L \left[\frac{\sin(k_0 L G)}{k_0 L G} \right] e^{-j(k_0 r - \frac{\pi}{4})} \quad (3.11)$$

B. FAR-FIELD ECHO WIDTH

Now that the scattered field is known, the echo width can be easily calculated using Equation (2.37). Substituting Equations (2.2) and (3.11) into Equation (2.37), and normalizing the echo width σ to the free space wavelength λ_0 , we obtain

$$\frac{\sigma}{\lambda} = \frac{1 + a^2}{2\pi} \left[2k_0 L \left(1 - \frac{D}{2[1 + a^2]} \right) \frac{\sin(k_0 LG)}{k_0 LG} \right]^2 \quad (3.12)$$

The above formula is for the bistatic echo width (receiver and transmitter are considered at different locations).

The monostatic case (transmitter and receiver at the same location) is a special case of the bistatic case, where the angle of incidence θ_0 is related with the observation angle θ by

$$\theta = 2\pi - \theta_0 \quad (3.13)$$

IV. SCATTERING FROM TRIANGULAR AND SINUSOIDAL PERFECTLY CONDUCTING SURFACE

In this chapter we investigate TM scattering from perfectly conducting triangular and sinusoidal surfaces. Expressions for the electric current induced for both the surfaces and the echo width for the sinusoidal case alone are developed. The sinusoidal surface is generally considered as a prototype surface for studying scattering from more complicated, rough surfaces. The scattering surface profiles are shown in Figure 4.

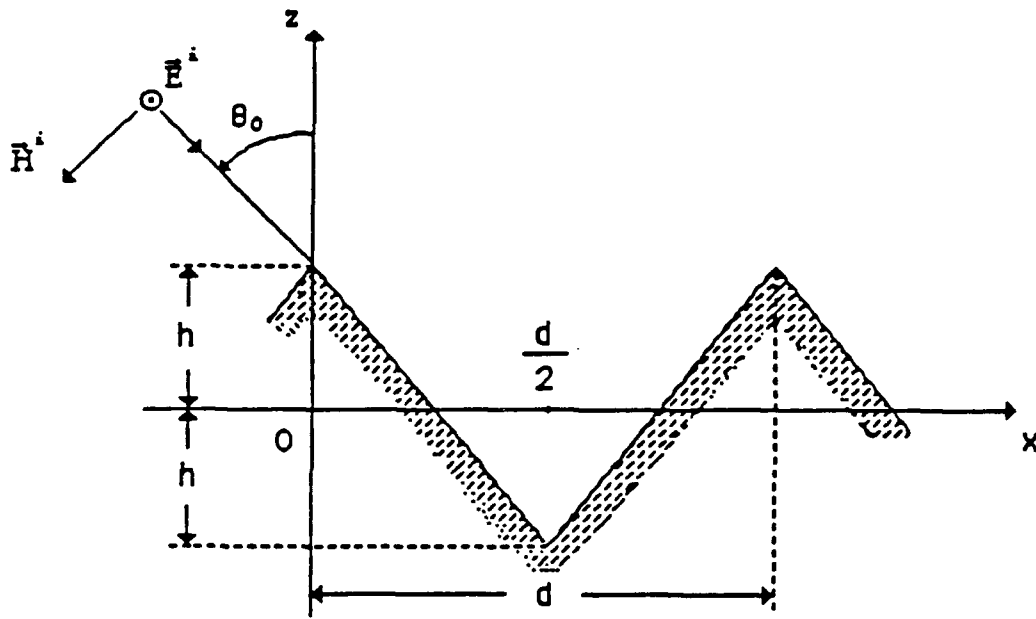
A. TRIANGULAR CASE

For the case of the triangular profile, as shown in Figure 4(a), the surface is described by

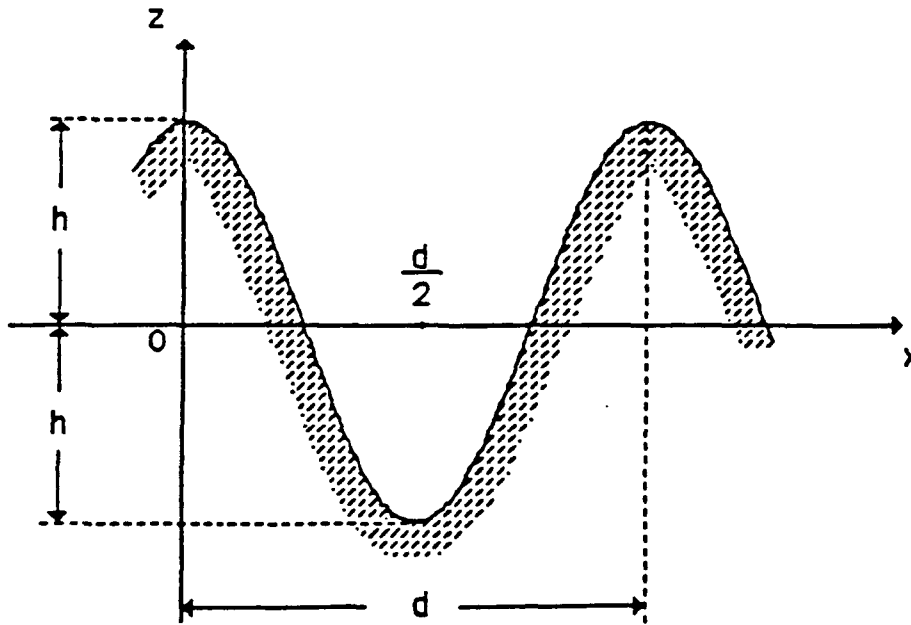
$$z(x) = h - \frac{4h}{d}x \quad , \quad 0 \leq x \leq \frac{d}{2} \quad (4.1a)$$

$$z(x) = -3h + \frac{4h}{d}x \quad , \quad \frac{d}{2} < x \leq d \quad (4.1b)$$

where d is the wavelength of the periodical surface. The expression for the normalized surface electric current density (Equation (2.36)) is simplified to



(a)



(b)

Figure 4 Profiles of periodic surfaces: (a) Triangular; (b) Sinusoidal.

$$\frac{H^{Tot}}{H^i} = U^i \left[\left(1 - \frac{\sin^2 \theta_0 + \frac{dz}{dx} \cos \theta_0 \left(2 \sin \theta_0 - \frac{dz}{dx} \cos \theta_0 \right)}{2 \left[1 + \left(\frac{dz}{dx} \right)^2 \right]} \right) + \frac{\frac{dz}{dx} \sin \theta_0 + \cos \theta_0}{\left[1 + \left(\frac{dz}{dx} \right)^2 \right]^{\frac{1}{2}}} \right] \quad (4.2)$$

where

$$\frac{dz}{dx} = -\frac{4h}{d} \quad , \quad 0 \leq x \leq \frac{d}{2} \quad (4.3a)$$

$$\frac{dz}{dx} = \frac{4h}{d} \quad , \quad \frac{d}{2} < x \leq d \quad (4.3b)$$

B. SINUSOIDAL CASE

The sinusoidal scattering surface profile (Fig. 4(b)) is described by

$$z(x) = h \cos(wx) \quad (4.4)$$

where $w = 2\pi/d$ and d is the wavelength of the sinusoidal surface. Hence

$$\frac{dz}{dx} = -hwsin(wx) \quad , \quad \frac{d^2z}{dx^2} = -hw^2 \cos(wx) \quad (4.5)$$

$$\frac{d\tau}{d\rho} = -hwsin\left(\frac{w\rho}{k_0}\right) \quad , \quad \frac{d^2\tau}{d\rho^2} = -\frac{hw^2}{k_0} \cos\left(\frac{w\rho}{k_0}\right) \quad (4.6)$$

and

$$k_0 z = k_0 h \cos(wx) \rightarrow \tau = k_0 h \cos\left(\frac{w\rho}{k_0}\right) \quad (4.7)$$

These quantities are used to express the normalized surface current induced on the surface and defined in Equation (2.36). The echo width of this surface is obtained in the following fashion.

Since the scattering surface is perfectly conducting with considerable thickness, the integral in Equation (2.28) is shown in Appendix B to be

$$\int_c F(\rho) \cdot Q(\rho) d\rho = \int_{\rho=-k_0 L}^{\rho=+k_0 L} \left(\frac{\partial U^s}{\partial n} + \frac{\partial U^i}{\partial n} \right) Q(\rho) d\rho \quad (4.8)$$

The far-zone, scattered field reduces to

$$U^s = V(r) \int_{\rho=-k_0 L}^{\rho=+k_0 L} \frac{1}{k_0 U^i} \left(\frac{\partial U^s}{\partial n} + \frac{\partial U^i}{\partial n} \right) U^i e^{jk_0 R \cos\psi} \left[1 + \left(\frac{d\tau}{d\rho} \right)^2 \right]^{\frac{1}{2}} d\rho \quad (4.9)$$

where

$$k_0 R \cos\psi = \rho \sin\theta + k_0 h \cos\left(\frac{w\rho}{k_0}\right) \cos\theta \quad (4.10)$$

The incident field on the surface of the scatterer is

$$U^i = e^{-j\left(\rho \sin\theta_0 - k_0 h \cos\left(\frac{w\rho}{k_0}\right) \cos\theta_0\right)} \quad (4.11)$$

For computational purposes it is convenient to rewrite the incident field as

$$U^i e^{jk_0 R \cos \psi} = e^{jT} \quad (4.12)$$

where

$$T = \rho (\sin \theta - \sin \theta_0) + k_0 h \cos \left(\frac{w\rho}{k_0} \right) (\cos \theta - \cos \theta_0) \quad (4.13)$$

Substituting these in Equation (4.9), we obtain

$$U^s = V(r) \int_{\rho = -k_0 L}^{\rho = +k_0 L} H(\rho) d\rho \quad (4.14)$$

where

$$H(\rho) = \frac{1}{k_0 U^i} \left(\frac{\partial U^s}{\partial n} + \frac{\partial U^i}{\partial n} \right) e^{jT} \left[1 + \left(\frac{d\tau}{d\rho} \right)^2 \right]^{\frac{1}{2}} \quad (4.15)$$

We normalize the limits of integration to the quantity $k_0 \cdot L$.

After some manipulation, Equation (4.14) reduces to

$$U^s = V(r) \left[\int_{-k_0 L}^0 H(\rho) d\rho + \int_0^{+k_0 L} H(\rho) d\rho \right] = U^s = V(r) \int_0^{k_0 L} [H(\rho) + H(-\rho)] d\rho \quad (4.16)$$

With the substitution $\rho = k_0 L u$, we get

$$U^s = V(r) k_0 L M \quad (4.17)$$

where

$$M = \int_0^1 [H(k_0 L u) + H(-k_0 L u)] du \quad (4.18)$$

Since a closed form formula has not been found for the scattered field, the integration in Equation (4.18) is performed numerically.

Once the quantity M has been calculated, the echo width σ normalized to the wavelength λ_0 is obtained from

$$\frac{\sigma}{\lambda_0} = |M|^2 \frac{(k_0 L)^2}{8\pi} \quad (4.19)$$

When normalized with respect to the length $(2L)$ of the scattering surface, the echo width is

$$\frac{\sigma}{2L} = |M|^2 \frac{k_0 L}{8} \quad (4.20)$$

V. NUMERICAL RESULTS

In this chapter, computed results for the induced electric surface current and the echo width are presented. In order to check our theory and computer codes, the results of the analytical solution (OSRC) are compared against the moment method, treated here as exact, and the physical optics solution. Details of these comparisons are presented in the following sections.

In all models where numerical results are presented, the following factors are considered:

1. The incident electromagnetic wave is a Transverse Magnetic plane wave incident in the x - z plane.
2. However, in an actual periodic surface the surface is infinite in the direction of periodicity, the width of the scattering surface considered here is finite and edge effects are ignored.
3. The induced electric current is plotted against the normalized distance (across one period of the periodic surface).
4. The resulting echo width σ is normalized to the wavelength λ_0 for the planar strip and to the surface total length $2L$ for the sinusoidal surface.
5. Curves presented for the exact and physical optics solution are taken from [Ref. 5] and [Ref. 6].

A. SURFACE CURRENT COMPARISONS

For a planar strip (Figure 3) of length $2L$, the magnitude of the surface current has a uniform distribution while the phase drops linearly across the strip, as shown in Figure 5, for incidence angles $\theta = 0^\circ, 30^\circ, 60^\circ, 90^\circ$. Notice that the current distribution does not exhibit any special behavior at the edges.

The magnitude of the surface current as a function of the incidence angle θ_0 for the OSRC solution as compared with the physical optics solution is shown in Figure 6. We can see that the agreement is remarkable between the two techniques for angles of incidence close to zero. However, the results deviate for angles of incidence exceeding 45° . For normal incidence the numerical (OSRC) results agreed with the exact solution to an accuracy better than 0.01 percent.

The comparisons for the sinusoidal surface between the numerical results generated by the present approach with both the exact solution and the physical optics approximation are shown in Figures 7, 8 and 9. Data pertaining to the latter two techniques are taken from [Ref. 5].

The surface currents obtained by all three methods for normal incidence are shown in Figures 7 and 8. Agreement of our solution with the other two is best for $h = 0.25\lambda_0$ and $d = 3.9\lambda_0$ (Figure 8), while for $h = 0.25\lambda_0$ and $d = 1.9\lambda_0$ (Figure 7) the numerical results deviate considerably from the

other two. The results seem to be closer to the physical optics approximation in both cases. The maximum deviation occurs at the peak and trough of the surface where the curvature is maximum. This is expected of the OSRC technique.

In general both outgoing and incoming waves exist on the surface of the scatterer. Millar [Ref. 7] has shown that for $2\pi h/d < 0.448$, the fields on the surface are predominantly of outgoing type. In the OSRC technique, a higher order radiation boundary condition is imposed directly on the surface of the scatterer. This implies that only outgoing waves have been assumed to exist on the surface of the scatterer. In the case of Figure 8, $2\pi h/d = 0.403$, which is less than the critical value of 0.448. Hence better agreement is seen for this case. However, in Figure 7, $2\pi h/d = 0.826$ resulting in poorer agreement.

In Figure 9 we present the results for the same geometry as in Figure 8, but for a 75° angle of incidence. The OSRC solution is not affected by the occurrence of shadowing as in the case of the physical optics. However, the results differ from the exact results especially in the central region (shadow region).

The current distributions on periodic surfaces with sinusoidal and triangular profiles (see Figure 4) are shown in Figures 10 through 15 represent. Each surface has a period $d = 0.2\lambda_0$, and a maximum amplitude $h = 0.1\lambda_0$ ($2\pi h/d = \pi$).

The angles of incidence considered are $\theta_0 = 0^\circ, 30^\circ$ and 60° . In each figure, the OSRC solution results are shown along with the exact solution as given in [Ref. 6]. It is seen from Figure 10 that the OSRC technique predicts an amplitude of approximately 6, both at the crest and the trough of a sinusoidal profile, whereas the exact solution predicts values of 5 and 0 at the crest and trough, respectively. The rather large deviation of the results at the trough is attributed to the presence of standing waves, which the OSRC technique fails to take into account.

For oblique incidences, OSRC technique predicts a jump discontinuity in the current magnitude at the center for triangular profiles as observed in Figures 13 through 15. This is due to the discontinuity of the surface slopes at these locations. The exact solution exhibits the proper edge condition whereas the OSRC fails to do so. A similar jump discontinuity is predicted by the physical optics [Ref. 6].

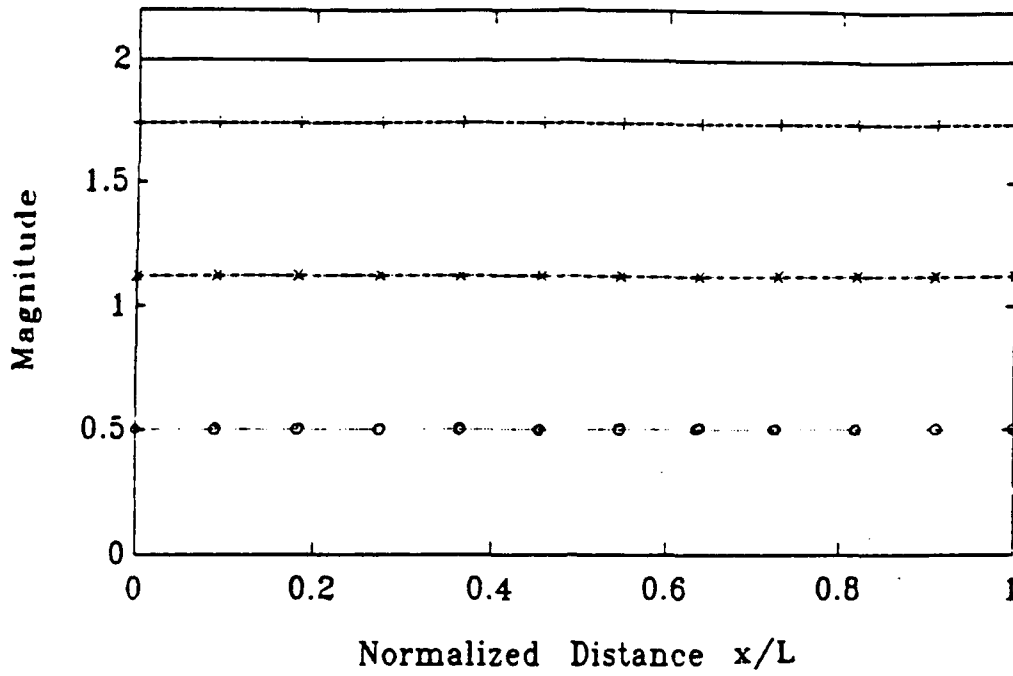
B. ECHO WIDTH COMPUTATIONS - COMPARISONS

The normalized monostatic echo width σ/λ_0 of a plane strip with length $2L$, as a function of the incidence angle θ_0 is shown in Figure 16. The normalized bistatic echo width σ/λ_0 , as a function of the observation angle θ , for $k_0L = 5$, $k_0L = 10$ and angle of incidence 0° and 60° is shown in Figure 17.

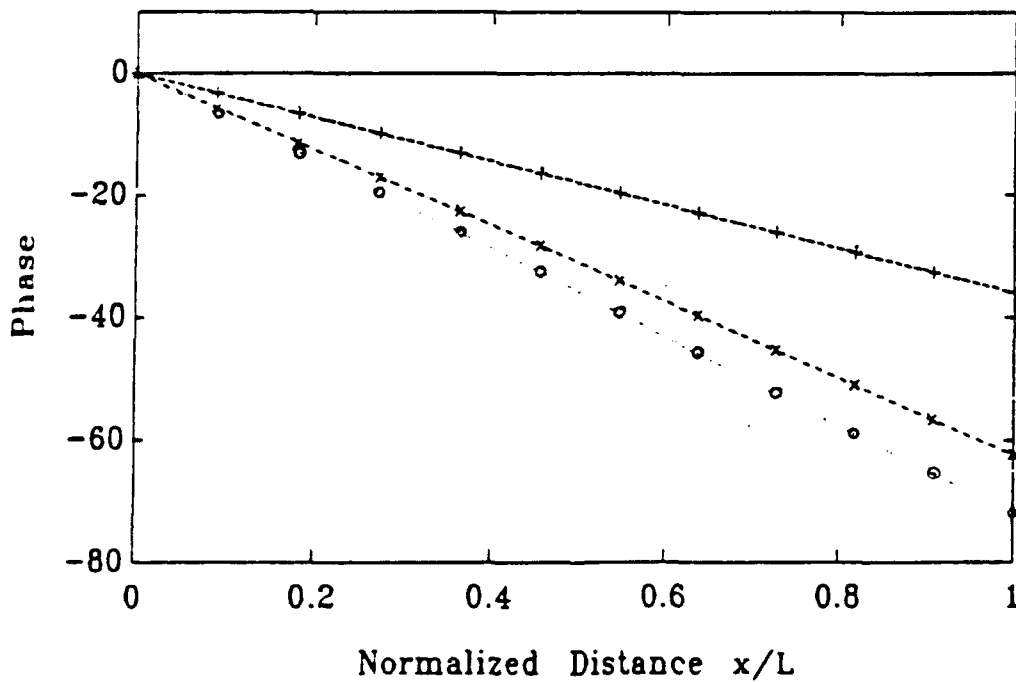
Figure 16 shows also the comparison between the numerical, the exact [Ref. 1], and the physical optics [Ref. 8] results. We see that we have a very good agreement (within 1 dB) with

the physical optics solution for angle of incidence up to 70° . Agreement with the exact solution is poor beyond 30° angle of incidence. The deviation from the exact solution, for larger angles of incidence, is probably due to edge currents that have been ignored in the formulation.

The normalized monostatic echo width $\sigma/2L$, of a sinusoidal surface of length $2L$ with parameters $h = 0.25\lambda_0$ and $d = 3.9\lambda_0$ is shown in Figure 18 while Figure 19 shows the normalized bistatic echo width $\sigma/2L$ of a sinusoidal surface with the same profile, for angle of incidence 0° and 60° . No comparison is made for the echo width of the sinusoidal surface.



(a)



(b)

Figure 5 Normalized surface current versus distance across a horizontal strip, $L = 0.2\lambda_0$. Lines: (—) - $\theta_0 = 0^\circ$; (---) - $\theta_0 = 30^\circ$; (x-) - $\theta_0 = 60^\circ$; (·o·) - $\theta_0 = 90^\circ$. (a) Magnitude; (b) Phase.

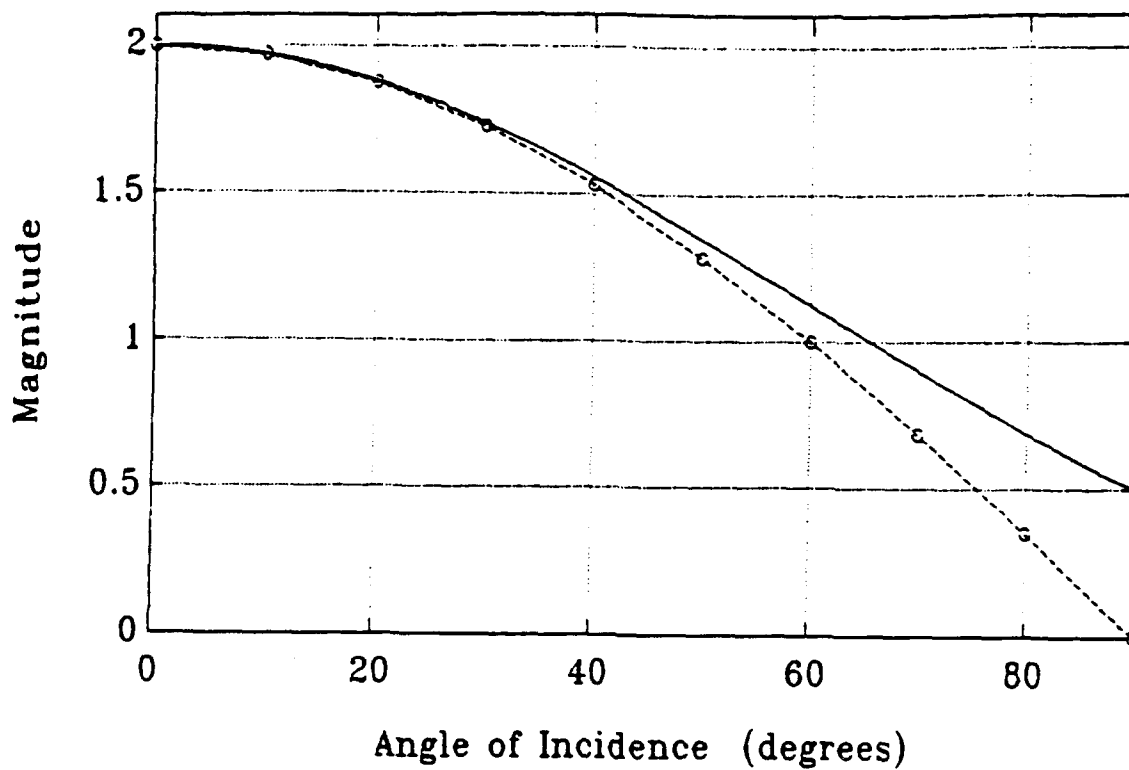
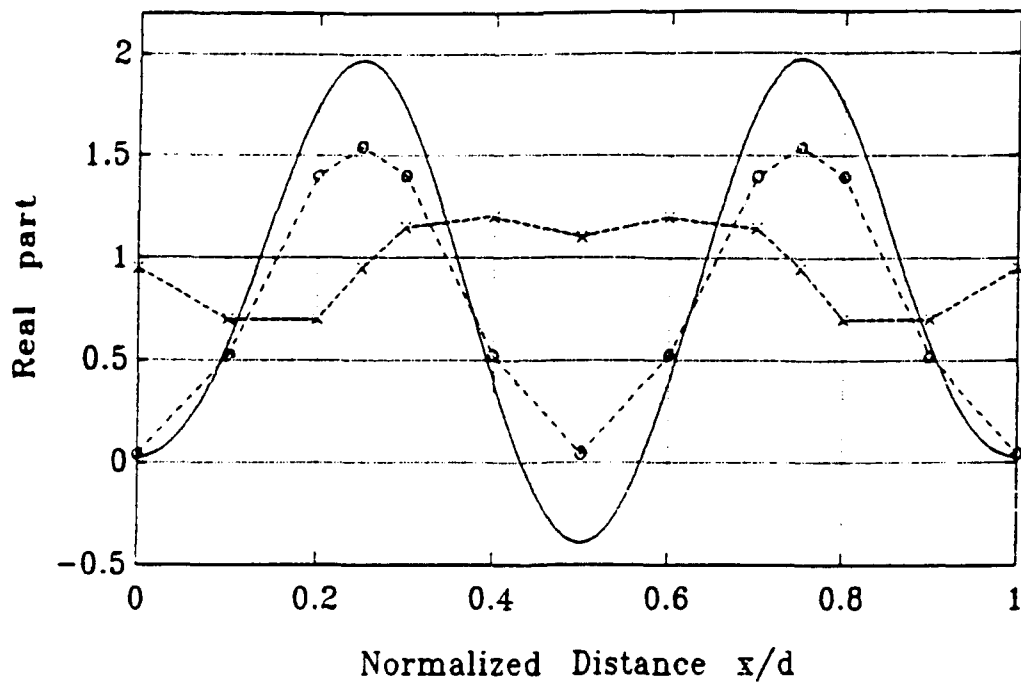
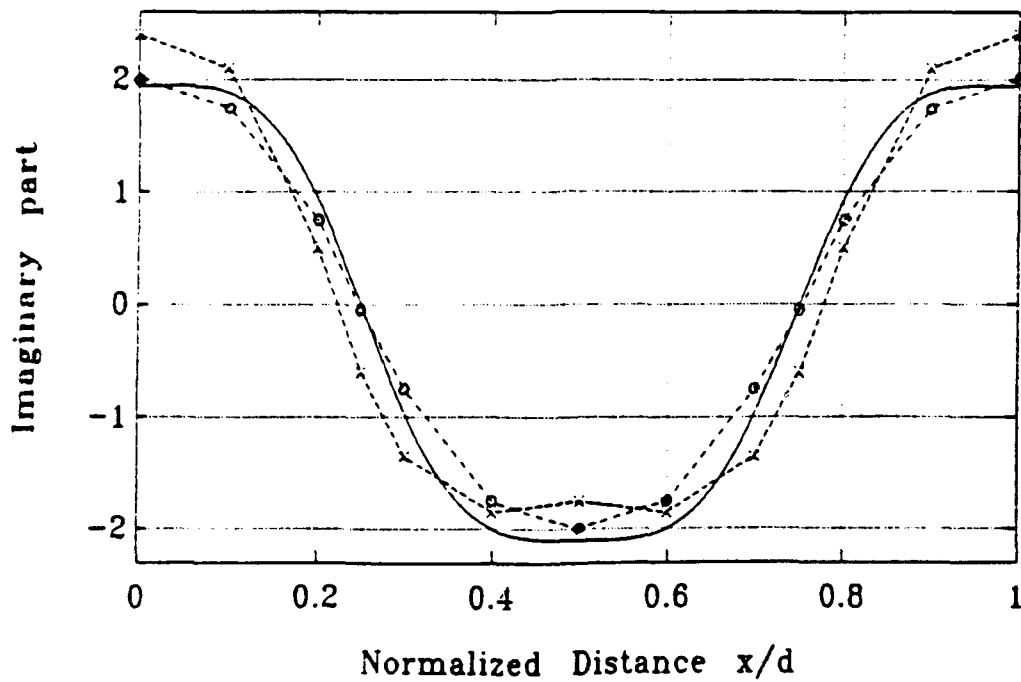


Figure 6 Normalized surface current versus angle of incidence θ_0 across a horizontal thin strip. Solid line: OSRC results; broken line: physical optics approximation.

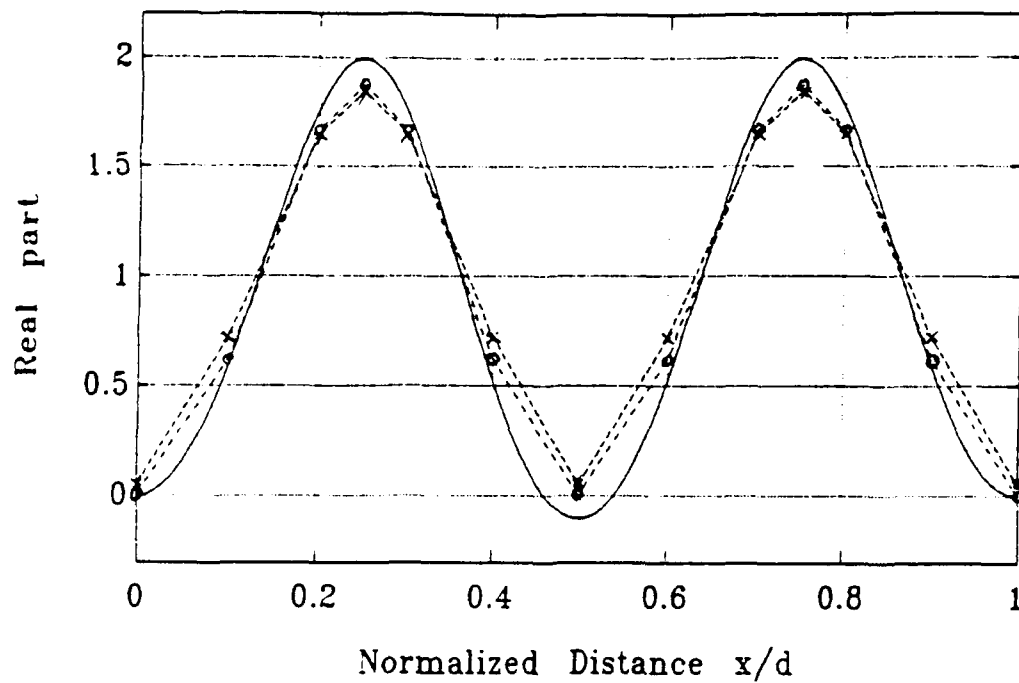


(a)

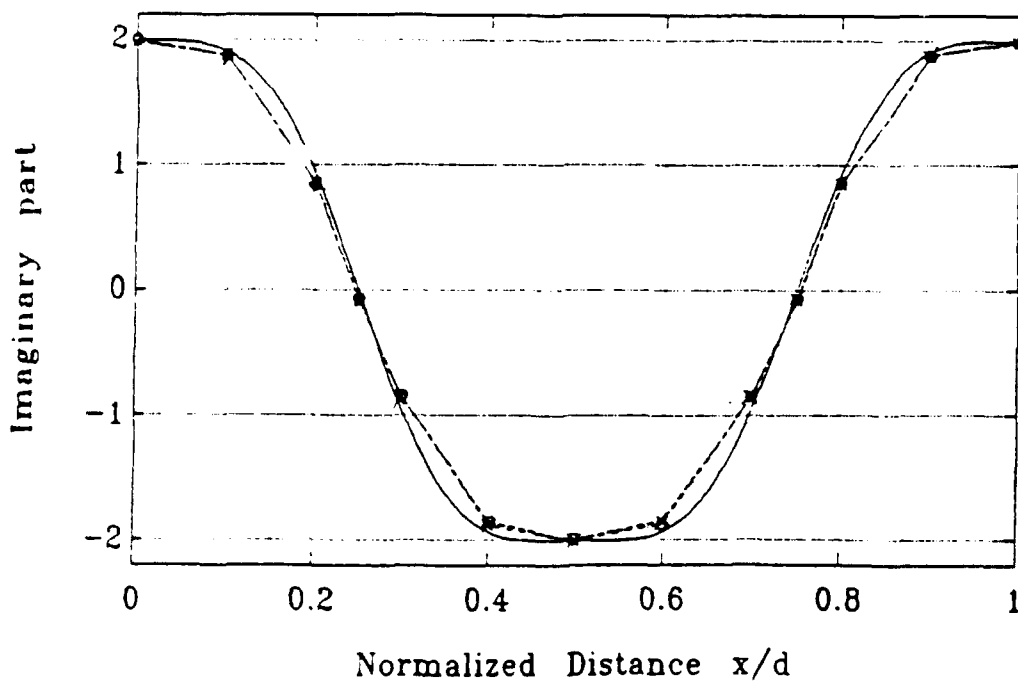


(b)

Figure 7 Normalized surface current versus distance across period of sinusoidal surface, $\theta_0 = 0^\circ$, $d = 1.9\lambda_0$, $h = 0.25\lambda_0$. Solid lines: OSRC results; broken lines: (-x-) - exact, (-o-) - physical optics.



(a)



(b)

Figure 8 Normalized surface current versus distance across period of sinusoidal surface, $\theta_0 = 0^\circ$, $d = 3.9\lambda_0$, $h = 0.25\lambda_0$. Solid lines: OSRC results; broken lines: (-x-) - exact, (-o-) - physical optics.

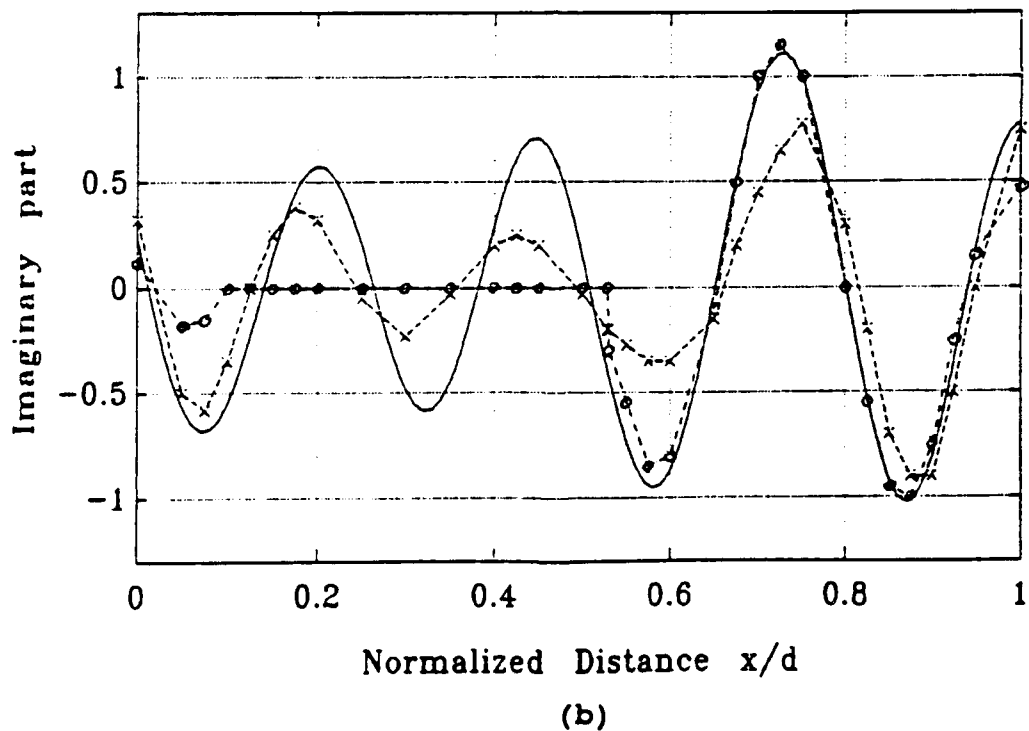
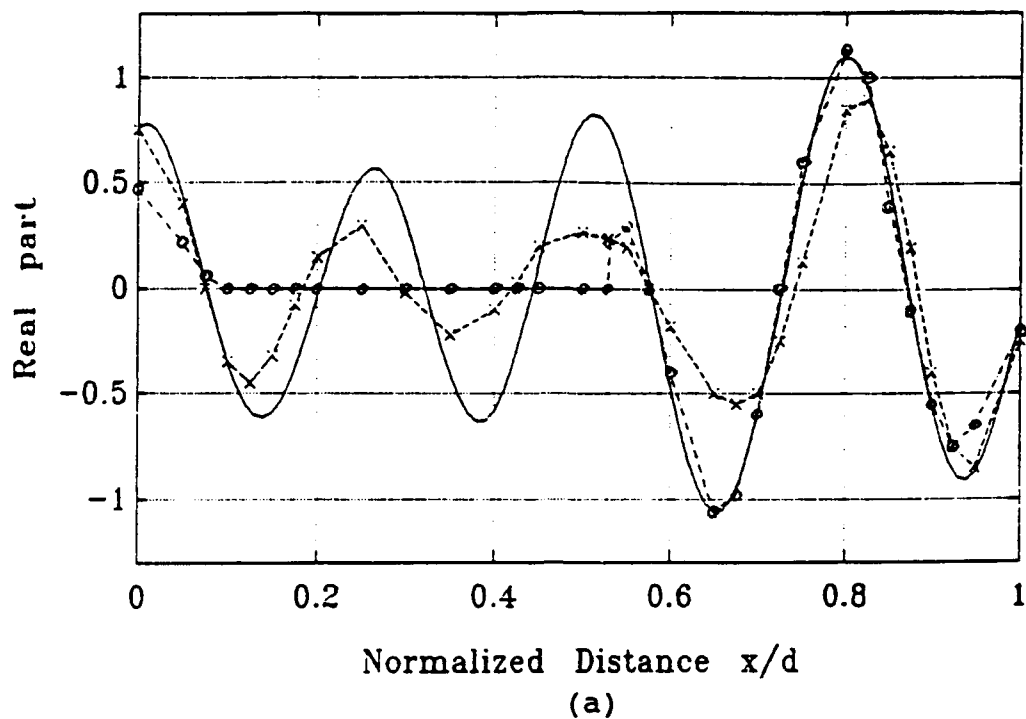
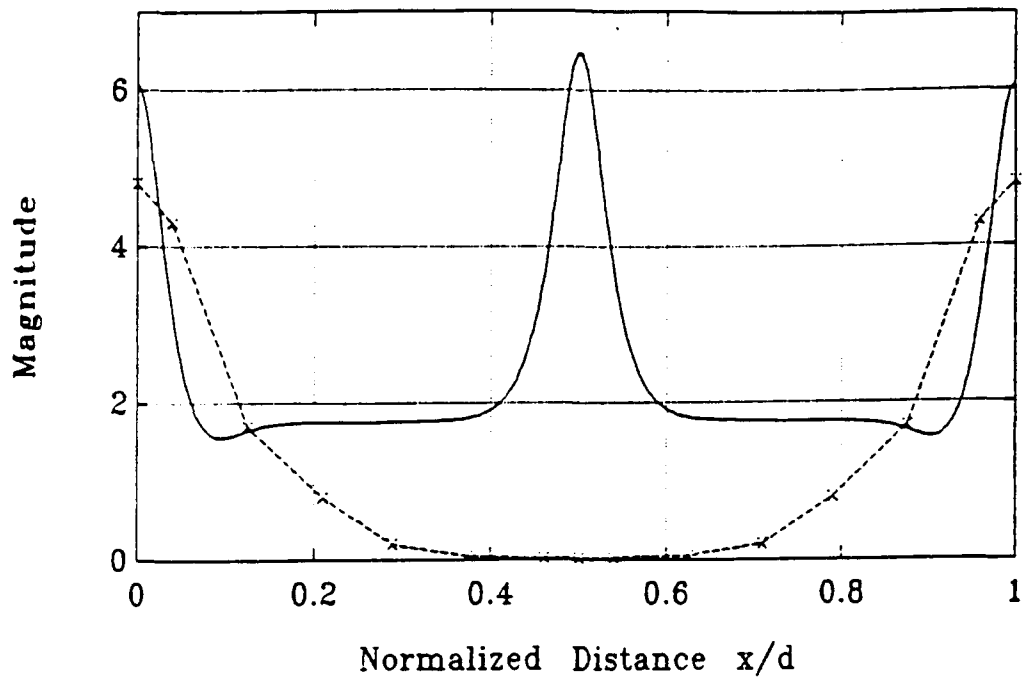
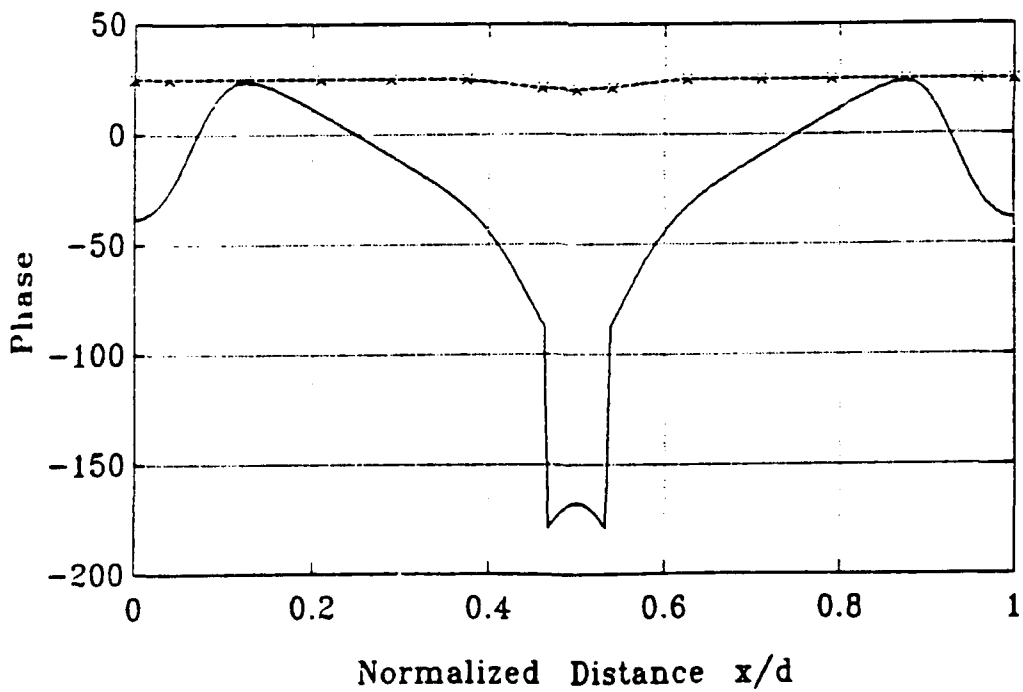


Figure 9 Normalized surface current versus distance across period of sinusoidal surface, $\theta_0 = 75^\circ$, $d = 3.9\lambda_0$, $h = 0.25\lambda_0$. Solid lines: OSRC results; broken lines: (-x-) - exact, (-o-) - physical optics.

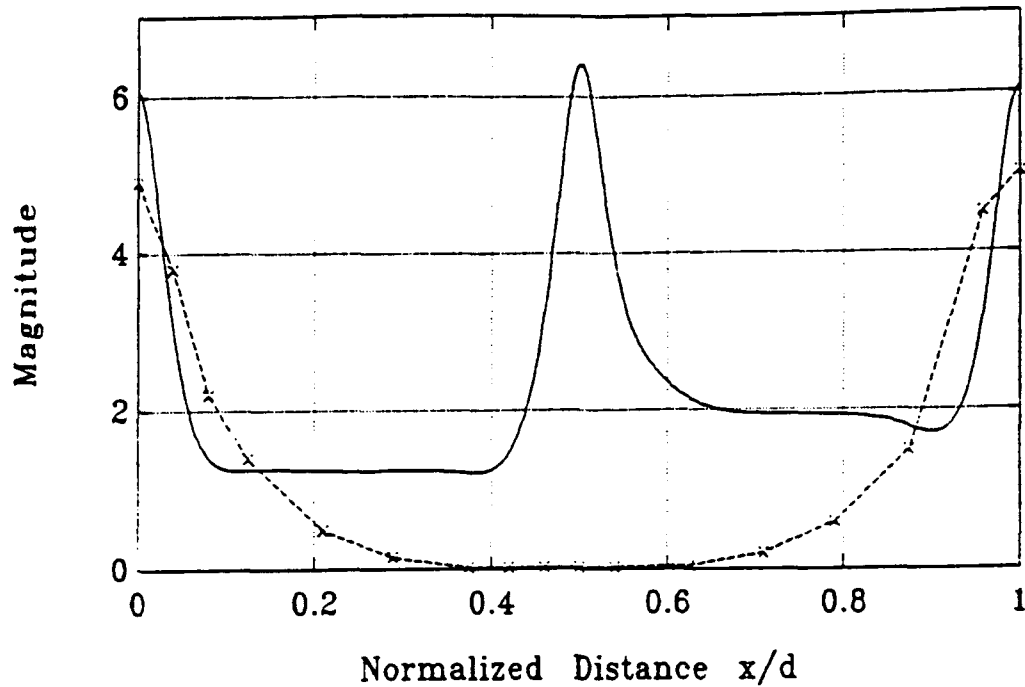


(a)

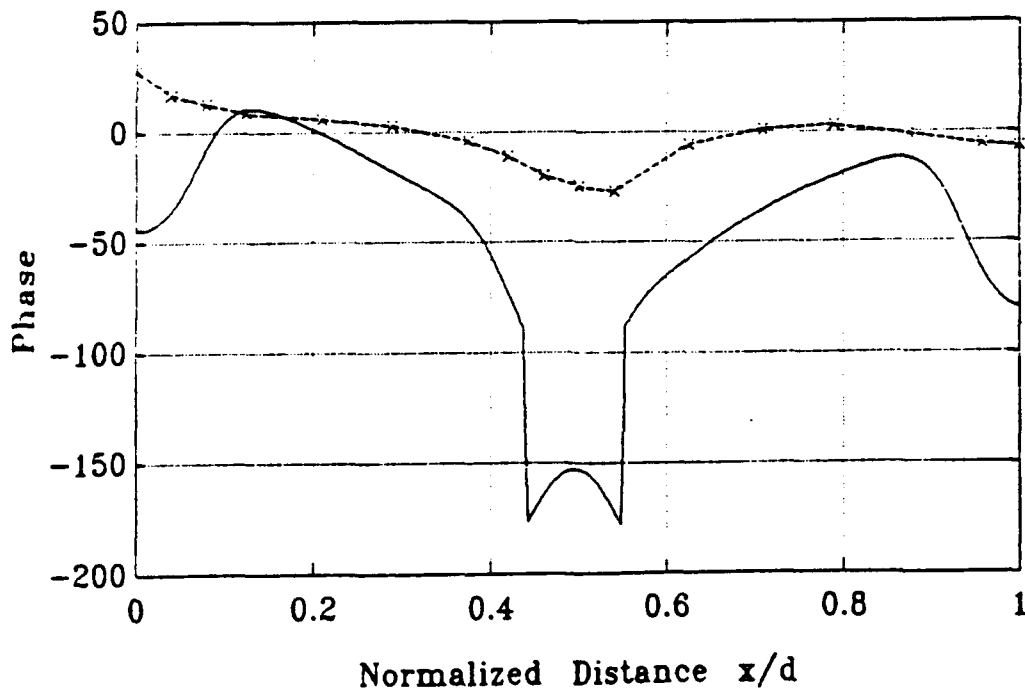


(b)

Figure 10 Normalized surface current versus distance across period of sinusoidal surface, $\theta_0 = 0^\circ$, $d = 0.2\lambda_0$, $h = 0.1\lambda_0$. Solid lines: OSRC results; broken lines: exact solution.

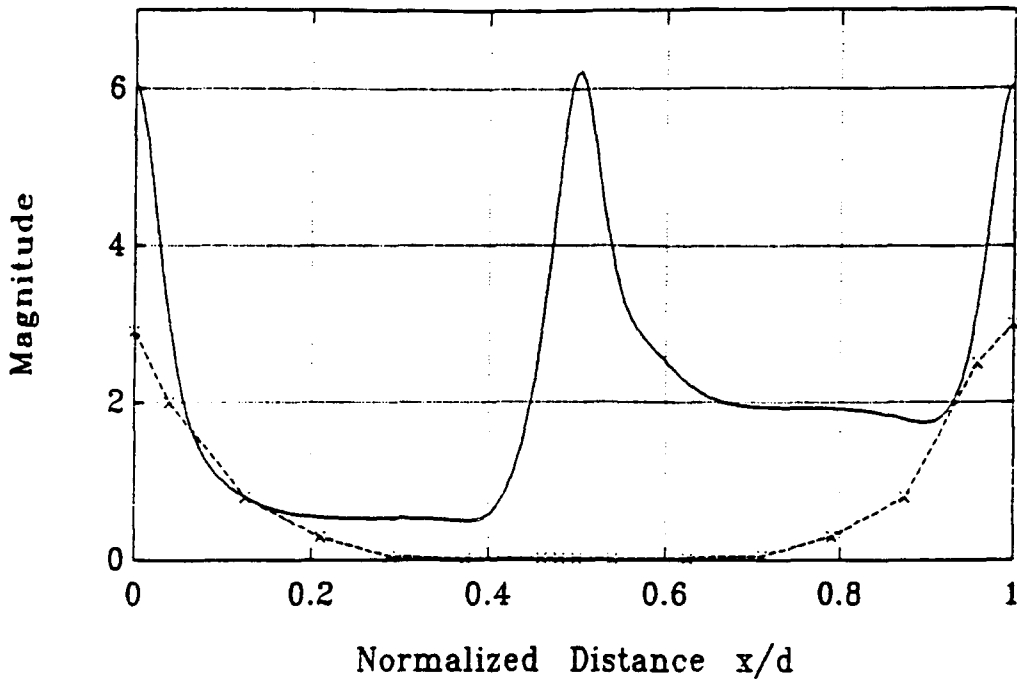


(a)

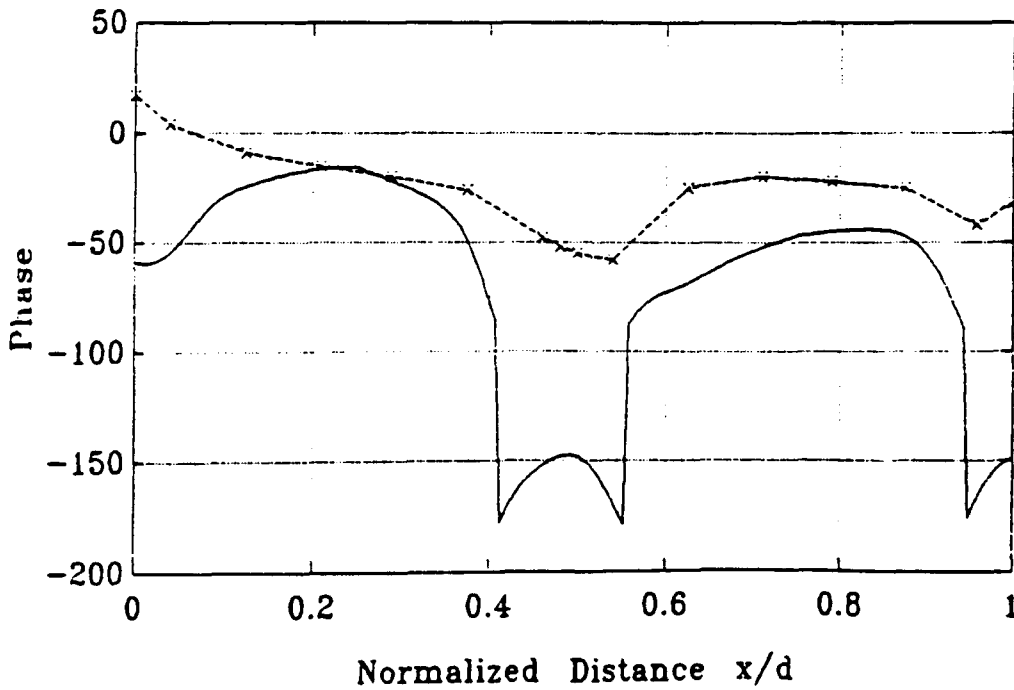


(b)

Figure 11 Normalized surface current versus distance across period of sinusoidal surface, $\theta_0 = 30^\circ$, $d = 0.2\lambda_0$, $h = 0.1\lambda_0$. Solid lines: OSRC results; broken lines: exact solution.

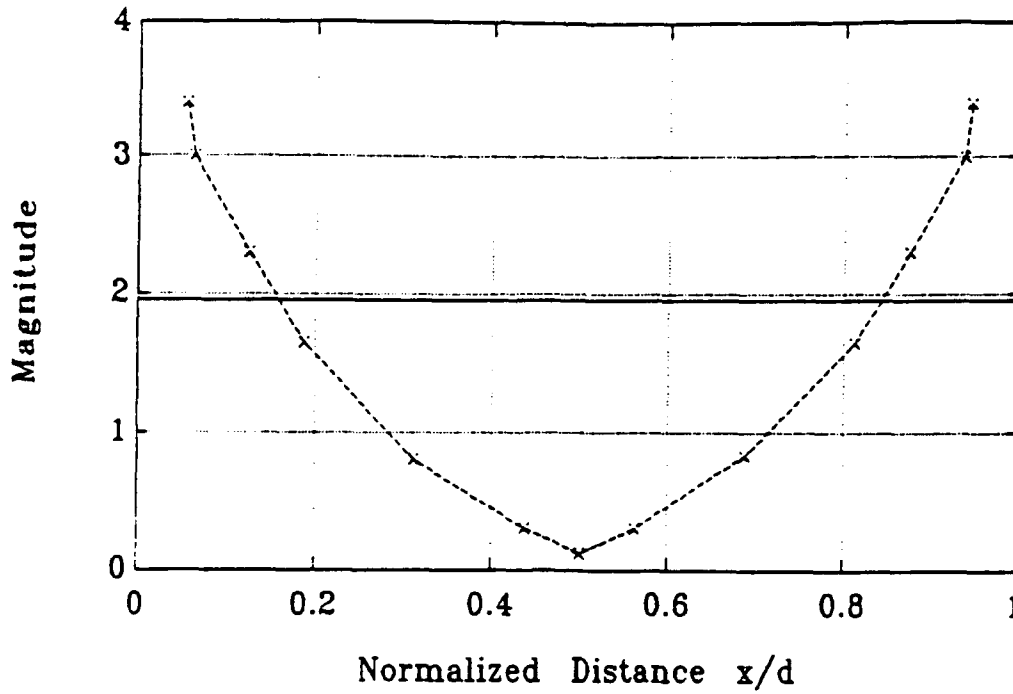


(a)

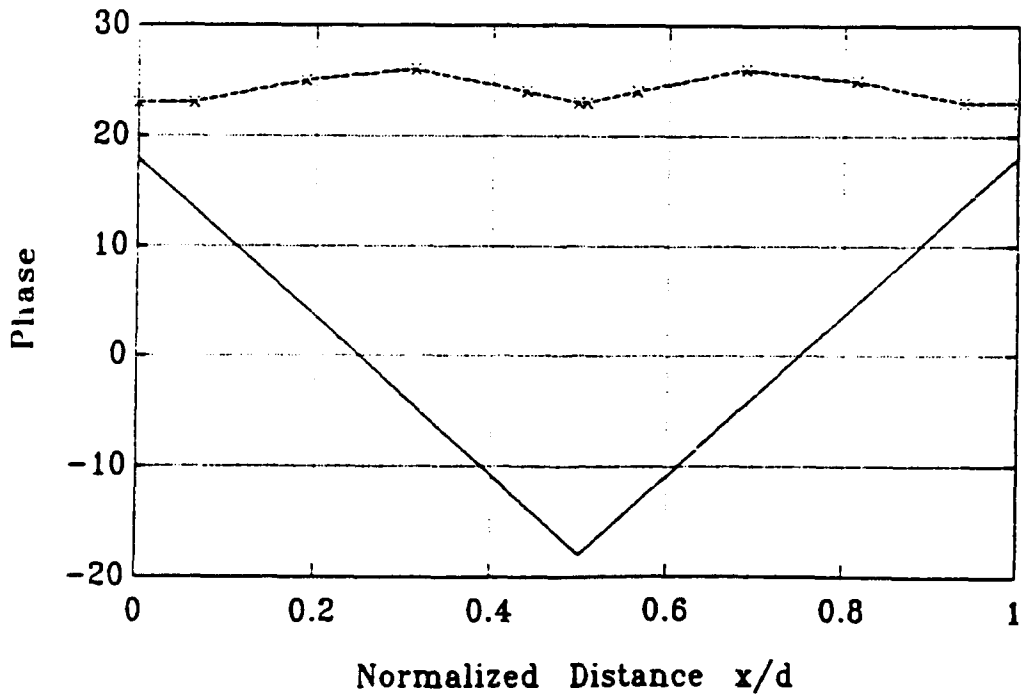


(b)

Figure 12 Normalized surface current versus distance across period of sinusoidal surface, $\theta_0 = 60^\circ$, $d = 0.2\lambda_0$, $h = 0.1\lambda_0$. Solid lines: OSRC results; broken lines: exact solution.



(a)



(b)

Figure 13 Normalized surface current versus distance across period of triangular surface, $\theta_0 = 0^\circ$, $d = 0.2\lambda_0$, $h = 0.1\lambda_0$. Solid lines: OSRC results; broken lines: exact solution.

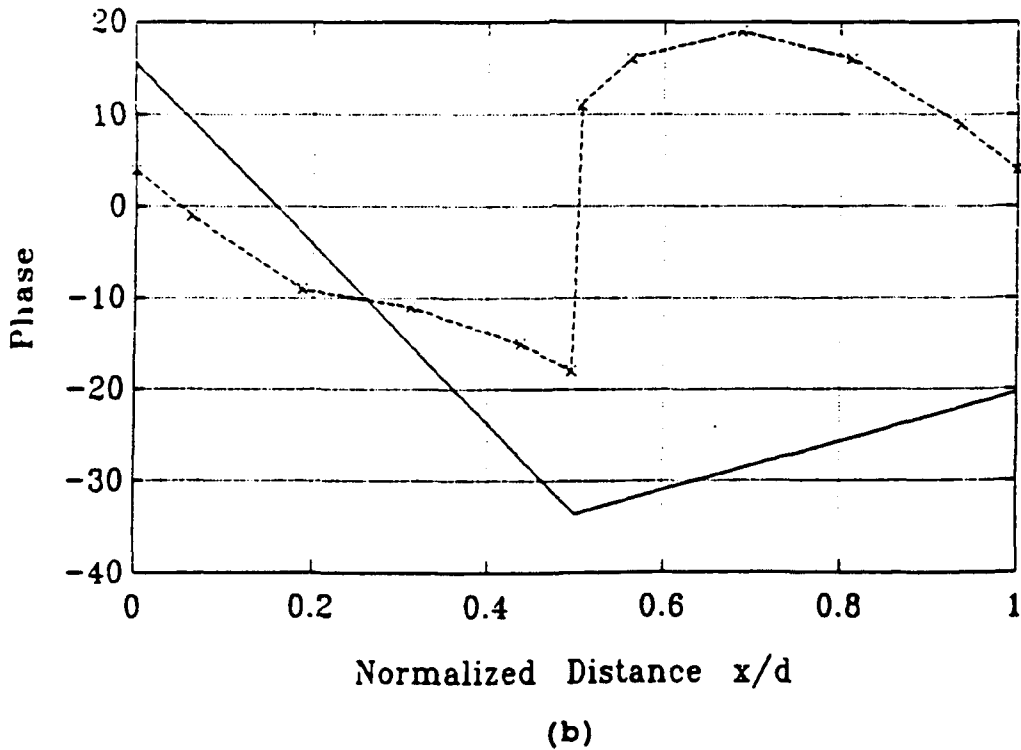
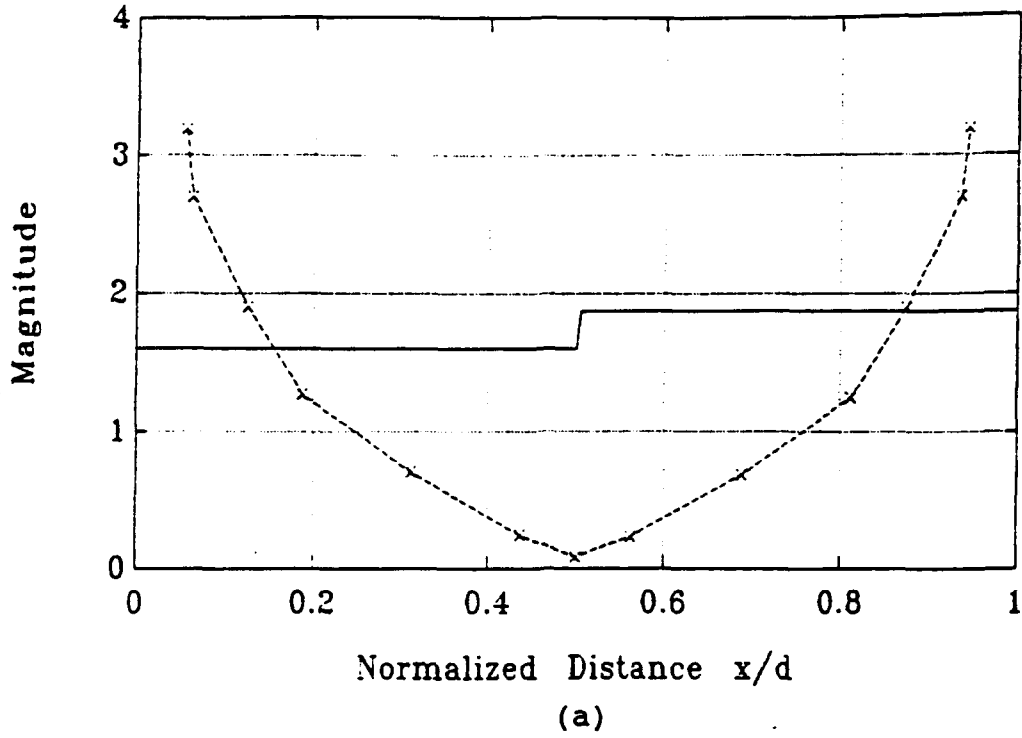
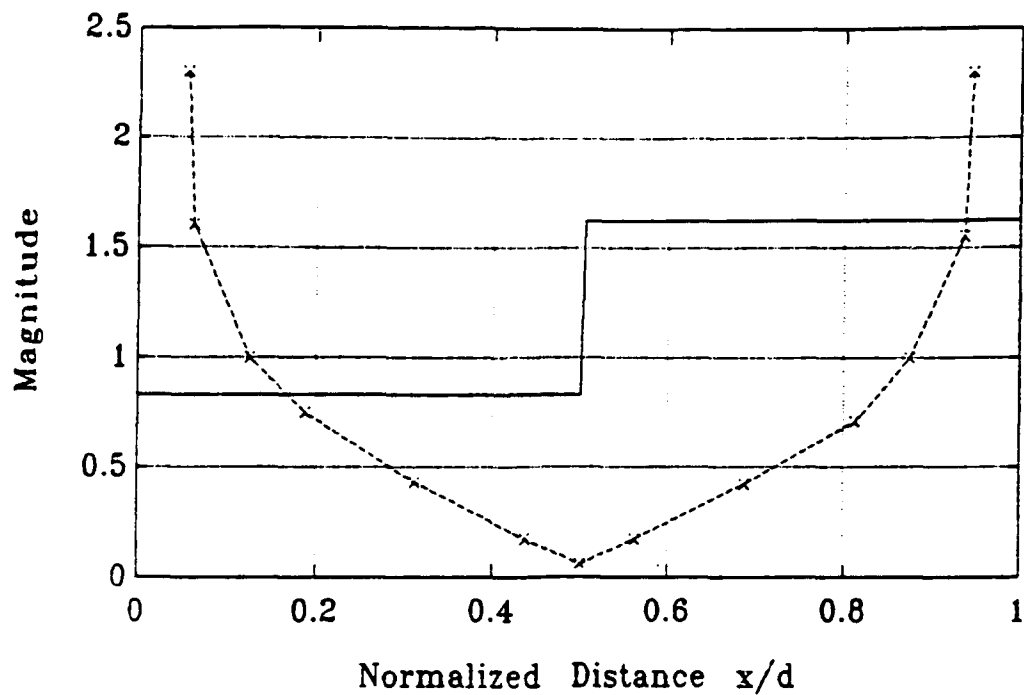
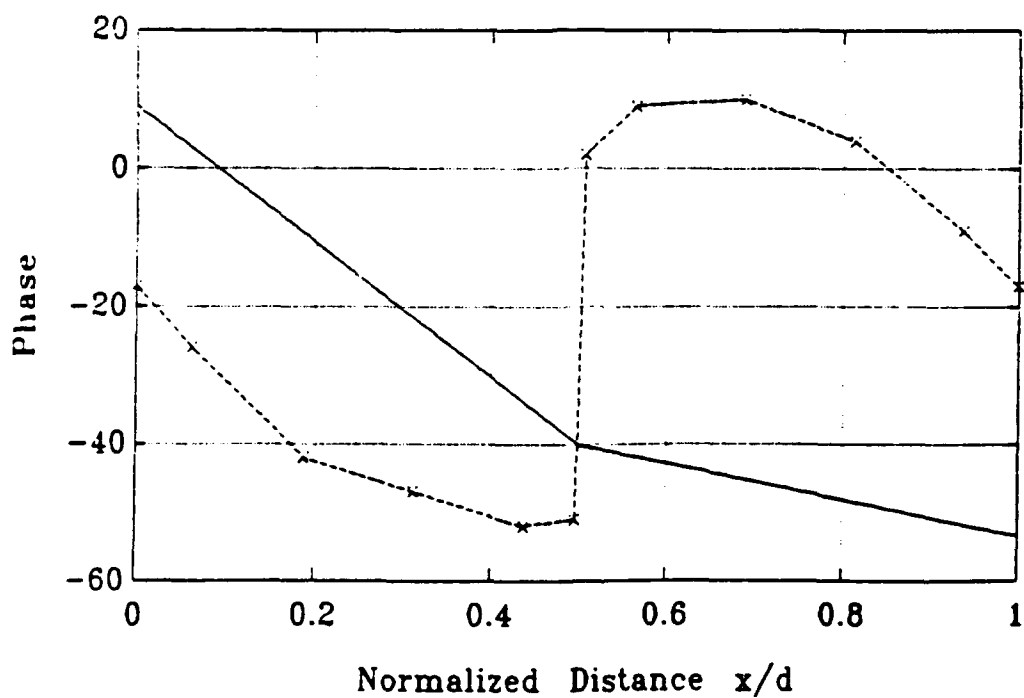


Figure 14 Normalized surface current versus distance across period of triangular surface, $\theta_0 = 30^\circ$, $d = 0.2\lambda_0$, $h = 0.1\lambda_0$. Solid lines: OSRC results; broken lines: exact solution.



(a)



(b)

Figure 15 Normalized surface current versus distance across period of triangular surface, $\theta_0 = 60^\circ$, $d = 0.2\lambda_0$, $h = 0.1\lambda_0$. Solid lines: OSRC results; broken lines: exact solution.

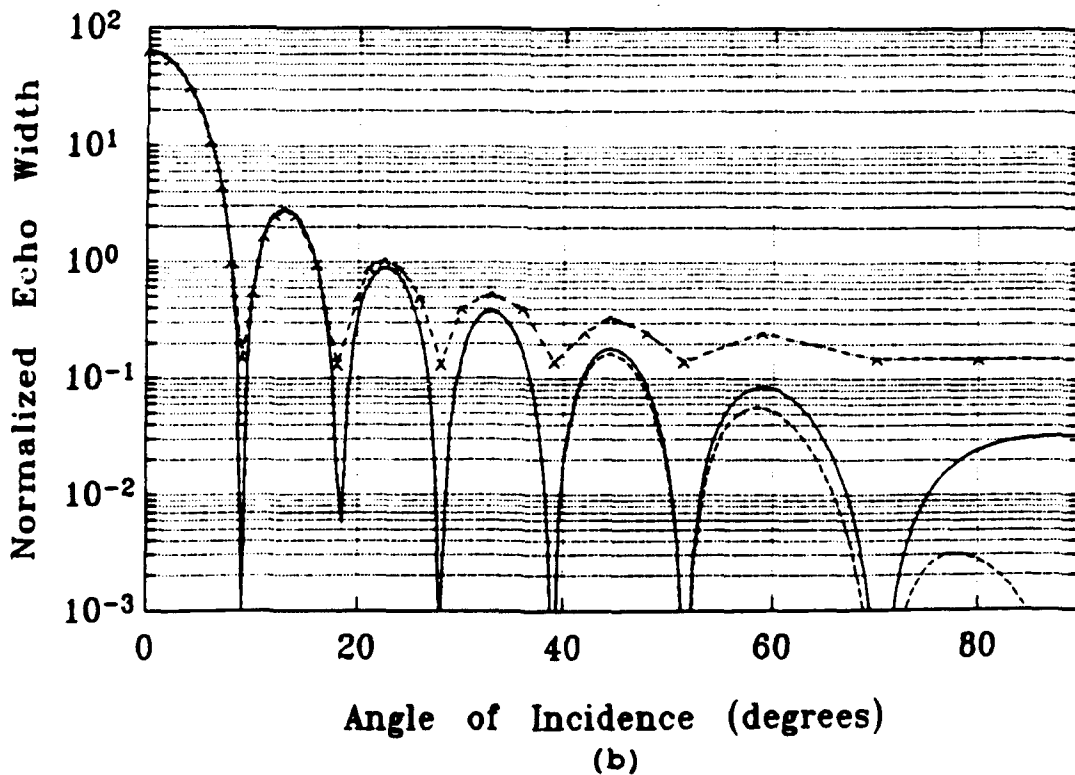
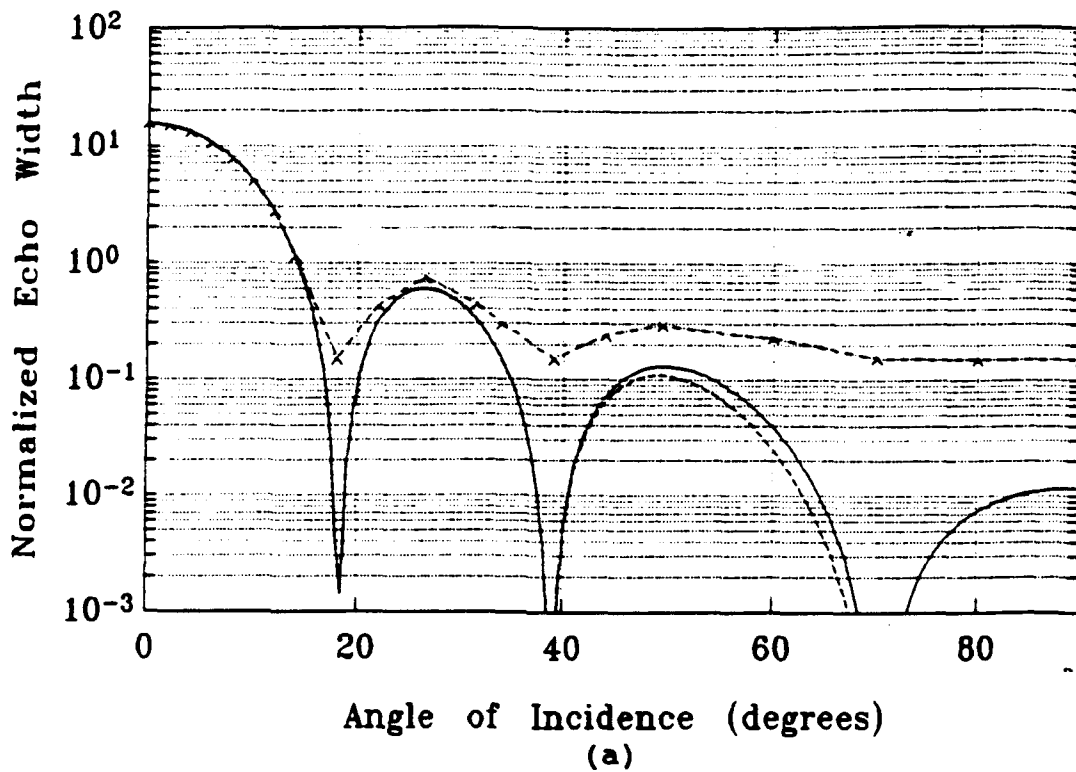


Figure 16 Normalized monostatic echo width σ/λ_0 , of horizontal conducting strip. Solid lines: OSRC results; broken lines: ($\cdot x$ -) - exact solution, (---) - physical optics. (a) $k_0L = 5$; (b) $k_0L = 10$.

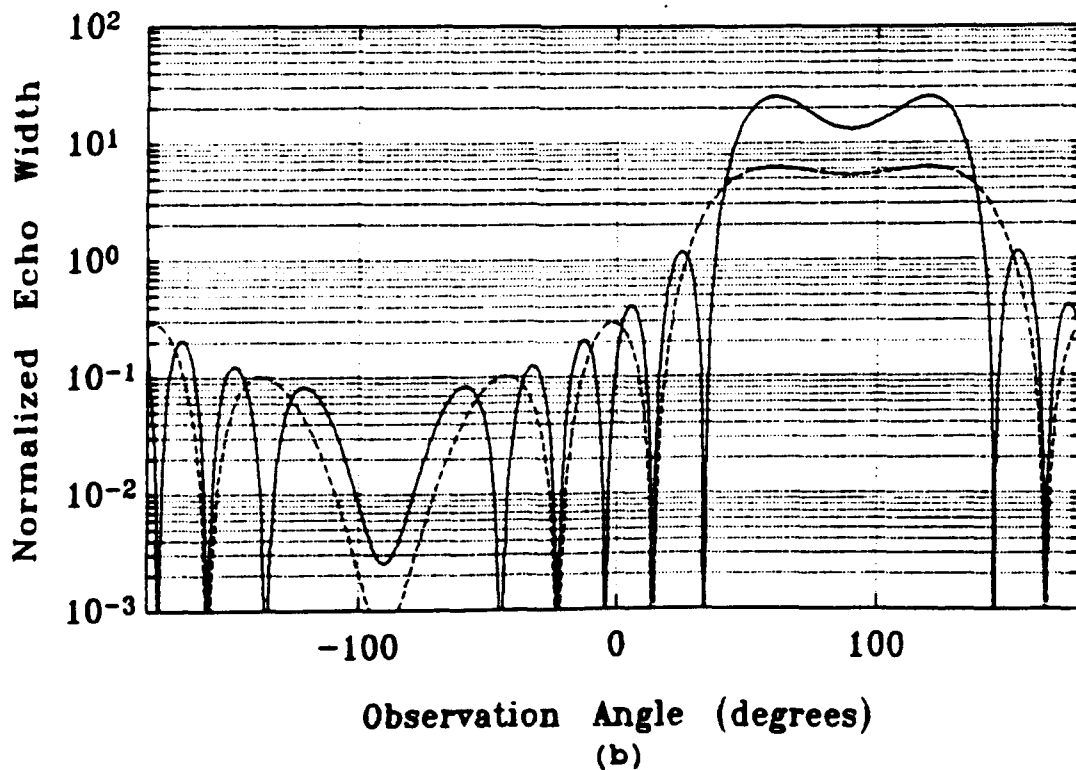
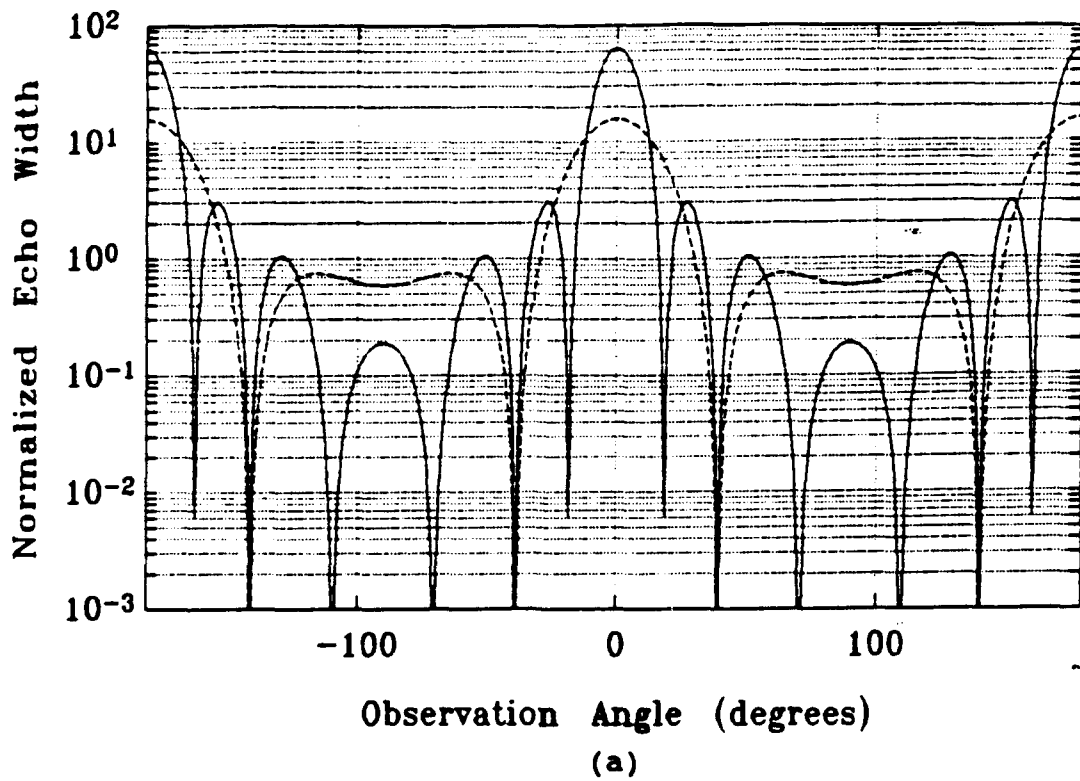


Figure 17 Normalized bistatic echo width σ/λ_0 of horizontal conducting strip - Numerical analysis (OSRC) results. Solid lines: $k_0L = 10$; broken lines: $k_0L = 5$. (a) $\theta_0=0^\circ$; (b) $\theta_0=60^\circ$.

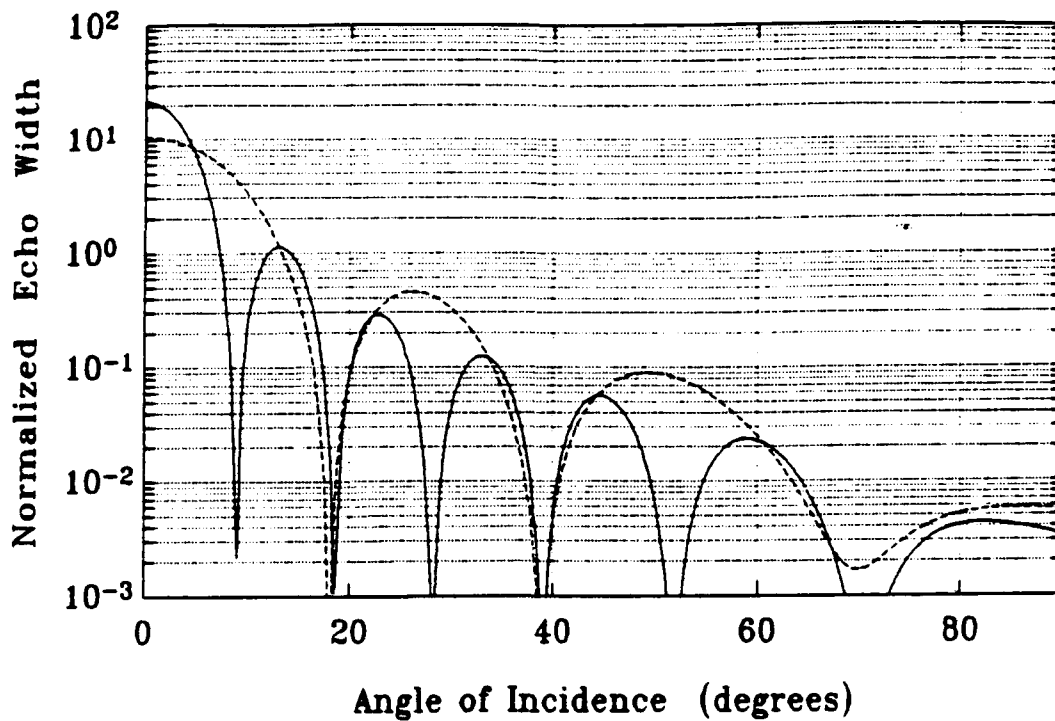


Figure 18 Normalized monostatic echo width $\sigma/2L$ of sinusoidal surface, $d = 3.9\lambda_0$, $h = 0.25\lambda_0$; - OSRC results -. Solid line: $k_0L = 10$; broken line: $k_0L = 5$.

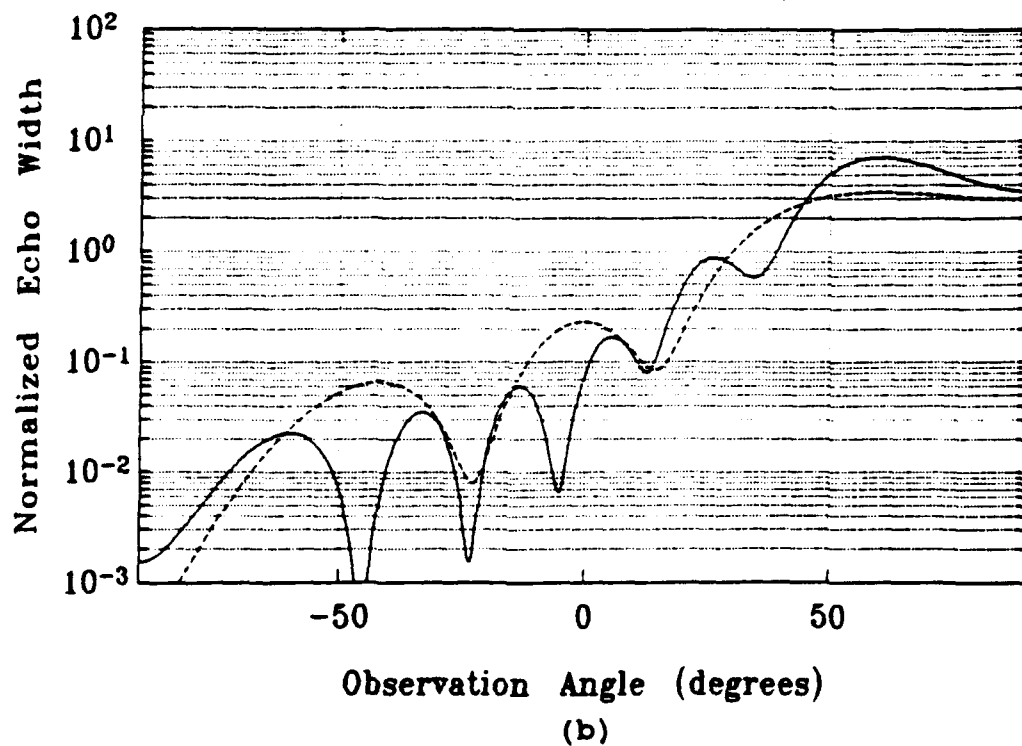
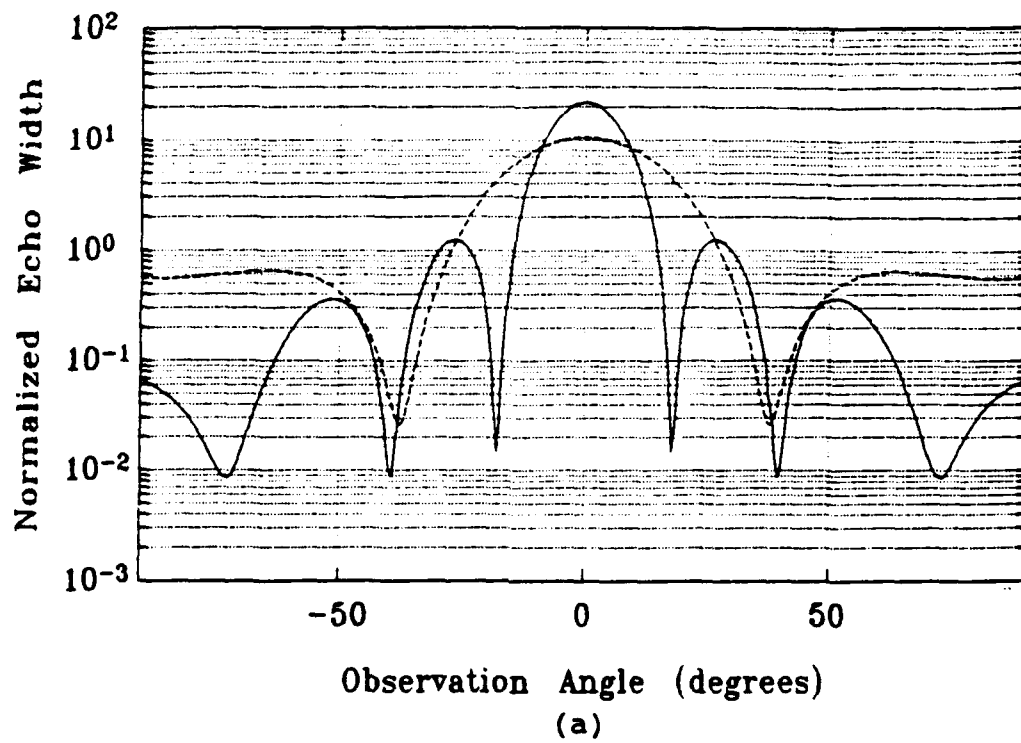


Figure 19 Normalized bistatic echo width $\sigma/2L$ of sinusoidal surface, $d = 3.9\lambda_0$, $h = 0.25\lambda_0$; - OSRC results -. Solid lines: $k_0L = 10$; broken lines: $k_0L = 5$. (a) $\theta_0 = 0^\circ$; (b) $\theta_0 = 60^\circ$.

VI. CONCLUSIONS

A. SUMMARY

Electromagnetic scattering from rough surfaces is hard to formulate and even harder to solve. In the On-Surface Radiation Boundary Condition a higher order radiation condition is imposed directly on the surface of the scatterer. The frequency-domain integral equation for the scattered field is reduced to just a line integral. This leads to substantial simplification of the problem. Analytical expressions are obtained for the surface scattered fields.

In this thesis, the OSRC method has been used to formulate electromagnetic scattering from a periodic rough, perfectly conducting surface. Transverse magnetic (TM) polarized, plane incident electromagnetic wave was considered throughout the whole formulation; the surface was considered of finite length, and edge effects were ignored.

Three different scattering surface profiles have been considered to test our formulation. The surface currents as well as the echo width of these surfaces were calculated by developing computer codes and the results were compared with results from the exact solution and the physical optics approximation.

For all the examined surfaces, the OSRC method predicts results somewhat between the two other solutions. For the

case of a thin strip, the OSRC results for the echo width are within 0.1 dB (except at nulls) of the exact solution for angles of incidence between 0° and 30° and deteriorating for larger angles of incidence. Actually OSRC results are more similar to the results given by physical optics.

For the cases of a triangular surface and a sinusoidal surface with parameters h and d such that $2\pi h/d > 0.448$, the OSRC results are not very accurate.

For the case of a sinusoidal surface, the validity of the OSRC results was shown to depend on surface profile parameters as well as the angle of incidence. When the quantity $2\pi h/d < 0.448$ and the angle of incidence is close to zero, the OSRC results are very accurate, while for larger angles of incidence it is somewhat closer to the exact solution than the physical optics one. Overall, the results of the OSRC technique seem to mimic those of the physical optics rather than the exact solution. This is clearly seen in all comparisons of current distribution and echo width.

B. RECOMMENDATIONS

With the basic theory for the TM case tested, we recommend the investigation of surface currents and echo width of other periodic surfaces. The formulation and the validation of the same problem, for the Transverse Electric (TE) case is another recommendation. Finally, how much the edge and the finite surface length affect the results needs to be investigated.

APPENDIX A

MATHEMATIC DERIVATIONS

In this Appendix we will derive the second partial derivative of the incident field with respect to the arc length on the scattering surface.

Let the electric field of the incident wave be denoted by an arbitrary function of the type $U = U(x, z)$. The surface of the scatterer is described by $z = z(x)$.

$$\frac{\partial U}{\partial s} = \frac{\partial U}{\partial x} \frac{dx}{ds} + \frac{\partial U}{\partial z} \frac{dz}{ds} = \left(\frac{\partial U}{\partial x} + \frac{\partial U}{\partial z} \frac{dz}{dx} \right) \frac{dx}{ds} \quad (\text{A.1})$$

where s is the arc length on the scattering surface.

Since

$$\frac{ds}{dx} = \left[1 + \left(\frac{dz}{dx} \right)^2 \right]^{\frac{1}{2}} \quad (\text{A.2})$$

we have then

$$\frac{\partial U}{\partial s} = \frac{\frac{\partial U}{\partial x} + \frac{\partial U}{\partial z} \frac{dz}{dx}}{\left[1 + \left(\frac{dz}{dx} \right)^2 \right]^{\frac{1}{2}}} \quad (\text{A.3})$$

If we name $W = \partial U / \partial s$, then

$$\frac{\partial^2 U}{\partial s^2} = \frac{\partial W}{\partial s} = \frac{\frac{\partial W}{\partial x} + \frac{\partial W}{\partial z} \frac{dz}{dx}}{\left[1 + \left(\frac{dz}{dx} \right)^2 \right]^{\frac{1}{2}}} \quad (\text{A.4})$$

It can be shown that

$$\frac{\partial W}{\partial x} = \frac{\left(\frac{\partial^2 U}{\partial x^2} + \frac{\partial^2 U}{\partial x \partial z} \frac{dz}{dx} + \frac{\partial U}{\partial z} \frac{d^2 z}{dx^2} \right)}{\left[1 + \left(\frac{dz}{dx} \right)^2 \right]^{\frac{1}{2}}} - \frac{\left(\frac{\partial U}{\partial x} + \frac{\partial U}{\partial z} \frac{dz}{dx} \right) \frac{dz}{dx} \frac{d^2 z}{dx^2}}{\left[1 + \left(\frac{dz}{dx} \right)^2 \right]^{\frac{3}{2}}} \quad (\text{A.5})$$

and

$$\frac{\partial W}{\partial z} = \frac{\left(\frac{\partial^2 U}{\partial z \partial x} + \frac{\partial^2 U}{\partial z^2} \frac{dz}{dx} \right)}{\left[1 + \left(\frac{dz}{dx} \right)^2 \right]^{\frac{1}{2}}} \quad (\text{A.6})$$

For the case of a plane incident wave

$$U^i = e^{-jk_0(x \sin \theta_0 - z \cos \theta_0)} \quad (\text{A.7})$$

we have

$$\frac{\partial U^i}{\partial x} = -jk_x e^{-j(k_x x - k_z z)} = -jk_x U^i \quad (\text{A.8})$$

$$\frac{\partial U^i}{\partial z} = -jk_z e^{-j(k_x x - k_z z)} = jk_z U^i \quad (\text{A.9})$$

$$\frac{\partial^2 U^i}{\partial x^2} = -k_x^2 e^{-j(k_x x - k_z z)} = -k_x^2 U^i \quad (\text{A.10})$$

$$\frac{\partial^2 U^i}{\partial z^2} = k_z^2 e^{-j(k_x x - k_z z)} = -k_z^2 U^i \quad (\text{A.11})$$

$$\frac{\partial^2 U^i}{\partial x \partial z} = \frac{\partial^2 U^i}{\partial z \partial x} = k_x k_z e^{-j(k_x x - k_z z)} \quad (\text{A.12})$$

where

$$k_x = k_0 \sin \theta_0, \quad k_z = k_0 \cos \theta_0 \quad (\text{A.13})$$

Finally, substituting Equations (A.5) through (A.13) in Equation (A.4), we get

$$\frac{\partial^2 U^i}{\partial s^2} = U^i \left[\frac{-k_0^2 \sin^2 \theta_0 + k_0^2 \frac{dz}{dx} \cos \theta_0 \left(2 \sin \theta_0 - \frac{dz}{dx} \cos \theta_0 \right) + j k_0 \frac{d^2 z}{dx^2} \cos \theta_0}{1 + \left(\frac{dz}{dx} \right)^2} + j k_0 \frac{(\sin \theta_0 - \frac{dz}{dx} \cos \theta_0) \frac{dz}{dx} \frac{d^2 z}{dx^2}}{\left[1 + \left(\frac{dz}{dx} \right)^2 \right]^2} \right] \quad (\text{A.14})$$

APPENDIX B

EVALUATION OF INTEGRALS

In this Appendix we present an approach for evaluating the line integrals with respect to the arc length that are encountered in Chapters 3 and 4 for the case of a planar strip and sinusoidal surface.

We are interested in evaluating an integral of the form $\int_C () d\rho$ where C is a conformal contour enclosing the surface.

We first consider the planar strip. The closed contour C around the scattering surface is considered to comprise of four contours C_1 , C_2 , C_3 and C_4 , as shown in Figure B1.

The contribution from contours C_3 and C_4 approaches zero for bounded integrands. The arc length s , as well as the differential arc length, ds , on the two contours C_1 and C_2 , with respect to the point A (Figure B1) is

$$s = \frac{L}{2} + x, \quad ds = dx \quad (\text{B.1})$$

on C_1 , and

$$s = L + \left(\frac{L}{2} - x \right), \quad ds = -dx \quad (\text{B.2})$$

on C_2 .

For computational purposes let us name the integral in Equation (2.5) as

$$I = \int_C \left(\frac{\partial U^s}{\partial n} + jk_0 U^i \cos \delta \right) ds \quad (\text{B.3})$$

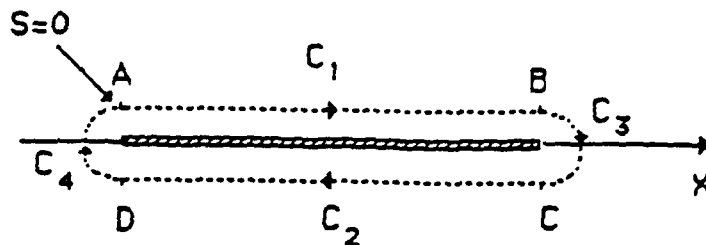


Figure B1. Integration contour for a thin strip.

We then have

$$I \approx \int_{c_1} \frac{\partial U^s}{\partial n_1} ds + \int_{c_2} \frac{\partial U^s}{\partial n_2} ds + jk_0 U^i \left(\int_{c_1} \hat{p} \cdot \hat{n}_1 ds + \int_{c_2} \hat{p} \cdot \hat{n}_2 ds \right) \quad (\text{B.4})$$

where \hat{n}_1 and \hat{n}_2 are the unit normal vectors outward to the contours C_1 and C_2 respectively.

Using Equations (B.1) and (B.2), we see that Equation (B.4) becomes

$$I \approx \int_{c_1} \frac{\partial U^s}{\partial n} dx - \int_{c_2} \frac{\partial U^s}{\partial n} dx + jk_0 U^i \left(\int_{c_1} \hat{p} \cdot \hat{n}_1 dx - \int_{c_2} \hat{p} \cdot \hat{n}_2 dx \right) \quad (\text{B.5})$$

Since $C_2 = -C_1$ and $\hat{n}_1 = -\hat{n}_2$, we have

$$I \approx \int_{c_1} \frac{\partial U^s}{\partial n} dx - \int_{-c_1} \frac{\partial U^s}{\partial n} dx + jk_0 U^i \left(\int_{c_1} \hat{p} \cdot \hat{n}_1 dx + \int_{-c_1} \hat{p} \cdot \hat{n}_1 dx \right) \quad (\text{B.6})$$

or

$$I = \int_{c_1} \frac{\partial U^s}{\partial n} dx + \int_{c_1} \frac{\partial U^s}{\partial n} dx + ik_0 U^i \left(\int_{c_1} \hat{r} \cdot \hat{n}_1 dx - \int_{c_1} \hat{r} \cdot \hat{n}_1 dx \right) \quad (\text{B.7})$$

Hence, for the case of a thin conducting strip, we have

$$\int_c \left(\frac{\partial U^s}{\partial n} + jk_0 U^i \cos \delta \right) ds = 2 \int_{c_1} \frac{\partial U^s}{\partial n} dx \quad (\text{B.8})$$

Let us now examine the case where the thickness of the scattering surface is no longer small, so that the second contour C_2 is considered to lie inside the conducting surface (Figure B2).

In this case we have

$$I = \int_{c_1+c_2} \frac{\partial U^s}{\partial n} ds + jk_0 U^i \left(\int_{c_1+c_2} \hat{r} \cdot \hat{n} ds \right) \quad (\text{B.9})$$

The second term in the above Equation (B.9) vanishes on the closed contour C_1+C_2 as shown previously. Inside a perfect conductor, the total magnetic field is zero. Hence on the contour C_2 , $\partial U^s / \partial n = -\partial U^i / \partial n$. Substituting these, we see that Equation (B.9) becomes

$$I = \int_{c_1} \frac{\partial U^s}{\partial n_1} ds + \int_{c_2} \frac{\partial U^s}{\partial n_2} ds = \int_{c_1} \frac{\partial U^s}{\partial n_1} ds - \int_{c_2} \frac{\partial U^i}{\partial n_2} ds \quad (\text{B.10})$$

Since $C_1 = -C_2$ and $\hat{n}_1 = -\hat{n}_2 = \hat{n}$, it follows that

$$\int_c \left(\frac{\partial U^s}{\partial n} + jk_0 U^i \cos \delta \right) ds = \int_{c_1} \frac{\partial U^s}{\partial n_1} ds + \int_{c_2} \frac{\partial U^i}{\partial n_2} ds = \int_{c_1} \left(\frac{\partial U^s}{\partial n} + \frac{\partial U^i}{\partial n} \right) ds \quad (\text{B.11})$$

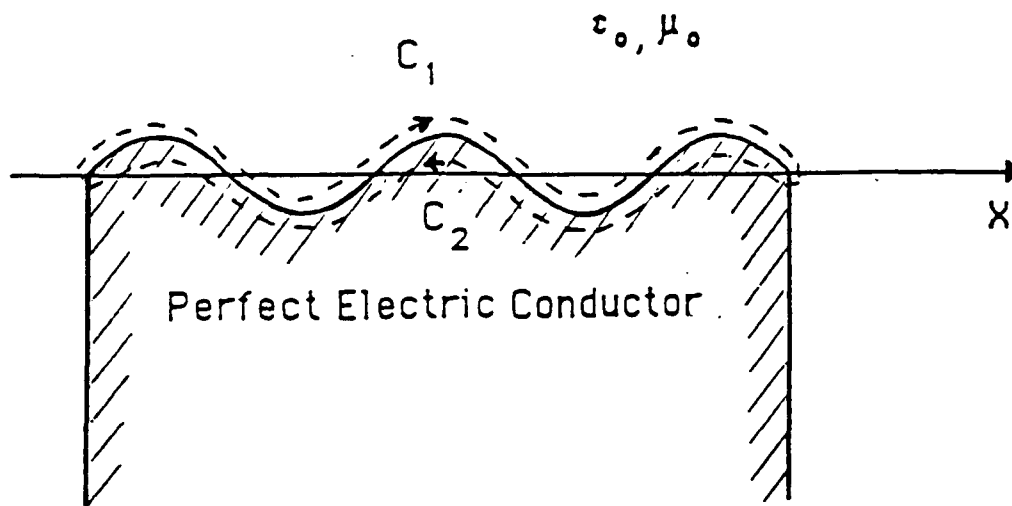


Figure B2. Integration contour for a thick surface.

APPENDIX C

PROGRAMS

In this Appendix we present the computer programs, all in FORTRAN language that are needed to perform the various calculations.

A. DISCUSSION

Programs STRIPCUR, SINUSCUR and TRIANCUR calculate the surface currents induced on the scattering surfaces, for a strip, sinusoidal and triangular profiles, respectively.

Programs STRIPMON and STRIPBI calculate the normalized monostatic and bistatic echo width, respectively, of thin, planar, perfectly conducting strip. Programs SINUSMON and SINUSBI calculate the same quantities but for a sinusoidal surface.

Since we deal with complex numbers most of the above mentioned programs contain subroutines to calculate the real (i.e. STRPREAL, SINREAL, FRSTREAL etc.) and the imaginary part (i.e. STRPIMAG, SINIMAG, MOODIMAG etc.) of a quantity and use subroutine PHASER to calculate the phase of this complex quantity.

Program TRIANCUR calculates the current distribution on the triangular surface, by examining separately the two halves of the surface, the first with negative slope (subroutines FRSTREAL, FRSTIMAG), and the second with positive slope (subroutines SCNDREAL, SCNDIMAG).

Programs SINUSMON and SINUSBI carry out the integration of

Equation (4.18), using Filon's method, as it is given by function subprogram FILON [Ref. 9]. To take advantage of the fast and accurate results of function FILON, we had to separate the even and the odd part of the examined function, as they are shown in subroutines MOEVREAL, MOEVIMAG, BIEVREAL, BIEVIMAG, and MOODREAL, MOODIMAG, BIODREAL, BIODIMAG respectively.

B. PROGRAM STRIPCUR

C THIS PROGRAM CALCULATES THE NORMALIZED SURFACE CURRENT
C ON A PLANAR, PERFECTLY CONDUCTING STRIP, DESCRIBED BY
C THE EQUATION: $z(x) = A * x$
C
C

C INPUT DATA:
C

C F = FREQUENCY IN GHz
C

C INCID = ELECTRIC FIELD ANGLE OF INCIDENCE (IN DEGREES),
C WITH RESPECT TO THE VERTICAL (+Z) AXIS
C

C A = SLOPE OF THE STRIP
C

C L = CONSIDERED LENGTH OF THE SURFACE
C

C M = NUMBER OF EQUIDISTANT POINTS BETWEEN $x=0$ AND
C $x=L$ WHERE OUR FUNCTION IS GOING TO BE
C EVALUATED.
C

C OUTPUT DATA:
C

C FREAL, FIMAG = REAL AND IMAGINARY PART RESPECTIVELY OF
C THE NORMALIZED SURFACE CURRENT
C

C AMAGNIT, PHASE = MAGNITUDE AND PHASE RESPECTIVELY OF
C THE NORMALIZED SURFACE CURRENT
C

C REAL K, INCID, INCR, L
C COMPLEX ZET
C

C COMMON K, A, THETA0
C

C OPEN (UNIT=11, FILE='STRIPCUR.DAT', FORM='FORMATTED',
C STATUS='UNKNOWN')
C

C READ(5,*) F, INCID, A, L, M
C

C PI = 4.*ATAN(1.)
C

C RAD = PI/180.
C

C THETA0 = INCID*RAD
C

C K = 20.*PI*F/3.
C

C INCR = L/M
C

C DO 100 X = 0., L, INCR
C

C DISTANCE = X/L
C

C FREAL = STRPREAL(X)
C

C FIMAG = STRPIMAG(X)
C

C ZET = CMPLX(FREAL, FIMAG)
C

C AMAGNIT = CABS(ZET)
C

```

        PHASE = PHASER(FREAL, FIMAG)
        WRITE(11,20) DISTANCE, FREAL, FIMAG, AMAGNIT, PHASE
20      FORMAT(1X, F12.6, 4X, F12.6, 4X, F12.6, 4X, F12.6,
&          4X, F12.6)
100    CONTINUE
        STOP
        END

C
C      *****
C      REAL FUNCTION STRPREAL(X)
C      *****
C
        REAL K, KC3
        COMPLEX J, POWER, FUSCAT, FUINC, UI, FUNC
        COMMON K, A, THETA0

C
        STHO = SIN(THETA0)
        CTHO = COS(THETA0)
        Z = A*X
        J = CMPLX(0.,1.)
        POWER = - J*K*(X*STHO - Z*CTHO)
        C = SQRT(1.+ A*A)
        D = (STHO)**2.+ A*CTHO*(2.*STHO - A*CTHO)
        FUSCAT = J*(1. - D/(2.*C*C))
        FUINC = J*((A*STHO + CTHO)/C)
        UI = CEXP(POWER)
        FUNC = - J*UI*(FUSCAT + FUINC)
        FUNCREAL = REAL(FUNC)
        RETURN
        END

C
C      *****
C      REAL FUNCTION STRPIMAG(X)
C      *****
C
        REAL K, KC3
        COMPLEX J, POWER, FUSCAT, FUINC, UI, FUNC
        COMMON K, A, THETA0

C
        STHO = SIN(THETA0)
        CTHO = COS(THETA0)
        Z = A*X
        J = CMPLX(0.,1.)
        POWER = - J*K*(X*STHO - Z*CTHO)
        C = SQRT(1.+ A*A)
        D = (STHO)**2.+ A*CTHO*(2.*STHO - A*CTHO)
        FUSCAT = J*(1. - D/(2.*C*C))
        FUINC = J*((A*STHO + CTHO)/C)
        UI = CEXP(POWER)
        FUNC = - J*UI*(FUSCAT + FUINC)
        FUNCIMAG = AIMAG(FUNC)
        RETURN

```


C. PROGRAM SINUSCUR

C THIS PROGRAM CALCULATES THE NORMALIZED SURFACE CURRENT
C ON A SINUSOIDAL, PERFECTLY CONDUCTING SURFACE, DESCRIBED
C BY THE EQUATION: $z(x) = H \cdot \cos([2 \cdot \pi / d] \cdot x)$
C
C

C INPUT DATA:
C

C F = FREQUENCY IN GHz
C

C INCID = ELECTRIC FIELD ANGLE OF INCIDENCE (IN DEGREES)
C WITH RESPECT TO THE VERTICAL (+Z) AXIS
C

C H, d = PARAMETERS OF THE SINUSOIDAL SURFACE
C

C M = NUMBER OF EQUIDISTANT POINTS BETWEEN X=0 AND
C X=d WHERE OUR FUNCTION IS GOING TO BE
C EVALUATED
C

C OUTPUT DATA:
C

C FREAL, FIMAG = REAL AND IMAGINARY PART RESPECTIVELY OF
C THE NORMALIZED SURFACE CURRENT
C

C AMAGNIT, PHASE = MAGNITUDE AND PHASE RESPECTIVELY OF
C THE NORMALIZED SURFACE CURRENT
C

C REAL K, INCID, INCR
C COPLEX ZET
C COMMON K, H, W, THETA0
C

C OPEN (UNIT=12, FILE='SINUSCUR.DAT', FORM='FORMATTED',
& STATUS='UNKNOWN')

C READ(5,*) F, INCID, H, d, M
C

PI = 4.*ATAN(1.)

W = 2.*PI/d

RAD = PI/180.

THETA0 = INCID*RAD

K = 20.*PI*F/3.

INCR = d/M

DO 100 X = 0., d, INCR

DISTANCE = X/d

FREAL = SINREAL(X)

FIMAG = SINIMAG(X)

ZET = CMPLX(FREAL, FIMAG)

AMAGNIT = CABS(ZET)

PHASE = PHASER(FREAL, FIMAG)

```

                WRITE(12,20) DISTANCE, FREAL, FIMAG, AMAGNIT, PHASE
20          FORMAT(1X, F12.6, 4X, F12.6, 4X, F12.6, 4X, F12.6,
&              4X, F12.6)
100 CONTINUE
      STOP
      END

C
C *****
C REAL FUNCTION SINREAL(X)
C *****
C
      REAL K, KC3
      COMPLEX J, POWER, BJKC3, DJE, FUSCAT, FUINC, UI, FUNC
      COMMON K, H, W, THETA0

C
      STHO = SIN(THETA0)
      CTHO = COS(THETA0)
      WX = W*X
      SW = SIN(WX)
      CW = COS(WX)
      Z = H*CW
      J = CMPLX(0.,1.)
      POWER = - J*K*(X*STHO - Z*CTHO)
      A = -H*W*SW
      B = -H*W*W*CW
      BA = ABS(B)
      C = SQRT(1.+ A*A)
      D = K*((STHO)**2.+ A*CTHO*(2.*STHO - A*CTHO))
      E = B*(CTHO + A*(STHO - A*CTHO)/(C*C))
      KC3 = K*C*C*C
      BJKC3 = BA + J*KC3
      DJE = D + J*E
      FUSCAT = BA/(2.*KC3)*(1 - BA/(4.*BJKC3)) + J
&          + C/(2.*BJKC3)*DJE
      FUINC = J*((A*STHO + CTHO)/C)
      UI = CEXP(POWER)
      FUNC = - J*UI*(FUSCAT + FUINC)
      FUNCREAL = REAL(FUNC)
      RETURN
      END

C
C *****
C REAL FUNCTION SINIMAG(X)
C *****
C
      REAL K, KC3
      COMPLEX J, POWER, BJKC3, DJE, FUSCAT, FUINC, UI, FUNC
      COMMON K, H, W, THETA0

C
      STHO = SIN(THETA0)
      CTHO = COS(THETA0)
      WX = W*X

```

```

SW = SIN(WX)
CW = COS(WX)
Z = H*CW
J = CMPLX(0.,1.)
POWER = - J*K*(X*STHO - Z*CTHO)
A = -H*W*SW
B = -H*W*W*CW
BA = ABS(B)
C = SQRT(1.+ A*A)
D = K*((STHO)**2.+ A*CTHO*(2.*STHO - A*CTHO))
E = B*(CTHO + A*(STHO - A*CTHO)/(C*C))
KC3 = K*C*C*C
BJKC3 = BA + J*KC3
DJE = D + J*E
FUSCAT = BA/(2.*KC3)*(1 - BA/(4.*BJKC3)) + J
&          + C/(2.*BJKC3)*DJE
FUINC = J*((A*STHO + CTHO)/C)
UI = CEXP(POWER)
FUNC = - J*UI*(FUSCAT + FUINC)
FUNCIMAG = AIMAG(FUNC)
RETURN
END

```

D. PROGRAM TRIANCUR

C THIS PROGRAM CALCULATES THE NORMALIZED SURFACE CURRENT
C ON A TRIANGULAR, PERFECTLY CONDUCTING SURFACE, DESCRIBED
C BY THE EQUATION:
C $z(x) = H - (4*H/d)*x$, for $0 < x < d/2$ (FIRST HALF)
C $z(x) = -3*H + (4*H/d)*x$, for $d/2 < x < d$ (SECOND HALF)
C
C
C

INPUT DATA:

C F = FREQUENCY IN GHz
C
C INCID = ELECTRIC FIELD ANGLE OF INCIDENCE (DEGREES),
C WITH RESPECT TO THE VERTICAL (+Z) AXIS
C
C H, d = PARAMETERS OF THE TRIANGULAR SURFACE
C
C M = NUMBER OF EQUIDISTANT POINTS BETWEEN x=0 AND
C x=d WHERE OUR FUNCTION IS GOING TO BE
C EVALUATED
C

OUTPUT DATA:

C FREAL, FIMAG = REAL AND IMAGINARY PART RESPECTIVELY OF
C THE NORMALIZED SURFACE CURRENT
C
C AMAGNIT, PHASE = MAGNITUDE AND PHASE RESPECTIVELY OF
C THE NORMALIZED SURFACE CURRENT
C

C REAL K, INCID, INCR
C COMPLEX ZET
C COMMON K, H, d, THETA0
C OPEN (UNIT=14, FILE='TRIANCUR.DAT', FORM='FORMATTED',
& STATUS='UNKNOWN')
C READ(5,*) F, INCID, H, d, M
C

C
C PI = 4.*ATAN(1.)
C RAD = PI/180.
C THETA0 = INCID*RAD
C K = 20.*PI*F/3.
C INCR = d/M
C DO 100 X = 0., d, INCR
C DISTANCE = X/d
C IF (DISTANCE.GE.0.0.AND.DISTANCE.LE.0.5) THEN
C FREAL = FRSTREAL(X)
C FIMAG = FRSTIMAG(X)
C ELSE

```

                FREAL = SCNDREAL(X)
                FIMAG = SCNDIMAG(X)
            ENDIF
            ZET = CMPLX(FREAL,FIMAG)
            AMAGNIT = CABS(ZET)
            PHASE = PHASER(FREAL, FIMAG)
            WRITE(14,20) DISTANCE, FREAL, FIMAG, AMAGNIT, PHASE
20          FORMAT(1X, F12.6, 4X, F12.6, 4X, F12.6, 4X, F12.6,
&              4X, F12.6)
100         CONTINUE
            STOP
            END

```

```

C
C *****
C REAL FUNCTION FRSTREAL(X)
C *****
C
REAL K, KC3
COMPLEX J, POWER, FUSCAT, FUINC, UI, FUNC
COMMON K, H, d, THETA0

C
STHO = SIN(THETA0)
CTHO = COS(THETA0)
A = - 4.*H/d
C = SQRT(1.+ A*A)
Z = H + A*X
J = CMPLX(0.,1.)
DI = (STHO)**2.+ A*CTHO*(2.*STHO - A*CTHO)
FUSCAT = J*(1. - DI/(2.*C*C))
FUINC = J*((A*STHO + CTHO)/C)
POWER = - J*K*(X*STHO - Z*CTHO)
UI = CEXP(POWER)
FUNC = - J*UI*(FUSCAT + FUINC)
FRSTREAL = REAL(FUNC)
RETURN
END

```

```

C
C *****
C REAL FUNCTION FRSTIMAG(X)
C *****
C
REAL K, KC3
COMPLEX J, POWER, FUSCAT, FUINC, UI, FUNC
COMMON K, H, d, THETA0

C
STHO = SIN(THETA0)
CTHO = COS(THETA0)
A = - 4.*H/d
C = SQRT(1.+ A*A)
Z = H + A*X
J = CMPLX(0.,1.)
DI = (STHO)**2.+ A*CTHO*(2.*STHO - A*CTHO)

```

```

FUSCAT = J*(1. - DI/(2.*C*C))
FUINC  = J*((A*STHO + CTHO)/C)
POWER  = - J*K*(X*STHO - Z*CTHO)
UI     = CEXP(POWER)
FUNC   = - J*UI*(FUSCAT + FUINC)
FRSTIMAG = AIMAG(FUNC)
RETURN
END

```

C
C
C
C

```

*****
REAL FUNCTION SCNDREAL(X)
*****

```

```

REAL K, KC3
COMPLEX J, POWER, FUSCAT, FUINC, UI, FUNC
COMMON K, H, d, THETA0

```

C

```

STHO = SIN(THETA0)
CTHO = COS(THETA0)
A = + 4.*H/d
C = SQRT(1.+ A*A)
Z = -3*H + A*X
J = CMPLX(0.,1.)
DI = (STHO)**2.+ A*CTHO*(2.*STHO - A*CTHO)
FUSCAT = J*(1. - DI/(2.*C*C))
FUINC  = J*((A*STHO + CTHO)/C)
POWER  = - J*K*(X*STHO - Z*CTHO)
UI     = CEXP(POWER)
FUNC   = - J*UI*(FUSCAT + FUINC)
SCNDREAL = REAL(FUNC)
RETURN
END

```

C
C
C
C

```

*****
REAL FUNCTION SCNDIMAG(X)
*****

```

```

REAL K, KC3
COMPLEX J, POWER, FUSCAT, FUINC, UI, FUNC
COMMON K, H, d, THETA0

```

C

```

STHO = SIN(THETA0)
CTHO = COS(THETA0)
A = + 4.*H/d
C = SQRT(1.+ A*A)
Z = -3*H + A*X
J = CMPLX(0.,1.)
DI = (STHO)**2.+ A*CTHO*(2.*STHO - A*CTHO)
FUSCAT = J*(1. - DI/(2.*C*C))
FUINC  = J*((A*STHO + CTHO)/C)
POWER  = - J*K*(X*STHO - Z*CTHO)
UI     = CEXP(POWER)

```

```
FUNC = - J*UI*(FUSCAT + FUINC)
SCNDIMAG = AIMAG(FUNC)
RETURN
END
```

E. PROGRAM STRIPMON

```
C THIS PROGRAM CALCULATES THE MONOSTATIC ECHO WIDTH
C OF A THIN, PLANAL, CONDUCTING STRIP OF LENGTH 2*L.
C
C INPUT DATA:
C
C F = FREQUENCY IN GHZ
C KOL = K0*L IS THE PRODUCT OF THE STRIP HALF
C LENGTH (L) TIMES K0 (K0=2*PI/WAVELENGTH)
C INCLIN = STRIP INCLINATION (IN DEGREES) WITH RESPECT
C TO THE HORIZONTAL (+X) AXIS
C STEP = ANGLE OF INCIDENSE INCREMENT
C
C OUTPUT DATA:
C
C ECHOMONO = NORMALIZED - WITH RESPECT TO THE WAVELENGTH -
C MONOSTATIC ECHO WIDTH AS A FUNCTION OF THE
C INCIDENT ANGLE THETA0, WHICH HERE (MONOSTATIC
C CASE) IS EQUAL TO: 2*PI - ANGLE OF INCIDENCE.
C
C REAL KOL, INCLIN
C OPEN (UNIT=1, FILE='STRIPMON.DAT', FORM='FORMATTED',
C & STATUS='UNKNOWN')
C READ(5,*) F, KOL, INCLIN, STEP
C
C PI = 4.*ATAN(1.)
C RAD = PI/180.
C A = TAN(INCLIN)
C C2 = 1. + A*A
C
C DO 100 QI = 0., 90., STEP
C THETA0 = QI*RAD
C THETAR = 2.*PI - THETA0
C STH0 = SIN(THETA0)
C CTH0 = COS(THETA0)
C STH = SIN(THETAR)
C CTH = COS(THETAR)
C
C D = (STH0)**2. + A*CTH0*(2.*STH0 - A*CTH0)
C G = STH - STH0 + ALPHA*(CTH + CTH0)
C
C ECHOMO=C2/(2.*PI)*(2.*(1.-D/(2.*C2))*SIN(KOL*G)/G)**2
C WRITE(1,*) QI, ECHOMO
100 CONTINUE
STCP
END
```

F. PROGRAM STRIPBI

```
C THIS PROGRAM CALCULATES THE BISTATIC ECHO WIDTH
C OF A THIN, PLANAL, CONDUCTING STRIP OF LENGTH 2*L.
C
C
C INPUT DATA:
C
C F = FREQUENCY IN GHz
C KOL = K0*L IS THE PRODUCT OF THE STRIP HALF
C LENGTH (L) TIMES K0 (K0=2*PI/WAVELENGTH)
C INCLIN = STRIP INCLINATION (IN DEGREES) WITH RESPECT
C TO THE HORIZONTAL (+X) AXIS
C INCID = ELECTRIC FIELD ANGLE OF INCIDENCE (IN DEGREES)
C WITH RESPECT TO THE VERTICAL (+Z) AXIS
C STEP = OBSERVATION ANGLE INCREMENT
C
C OUTPUT DATA:
C
C ECHOBI = NORMALIZED BISTATIC ECHO WIDTH AS A
C FUNCTION OF THE OBSERVATION ANGLE, THETA,
C FOR A GIVEN INCIDENT ANGLE
C
C
C REAL KOL, INCLIN, INCID
C OPEN (UNIT=2, FILE='STRIPBI.DAT', FORM='FORMATTED',
C & STATUS='UNKNOWN')
C READ(5, *) F, KOL, INCLIN, INCID, STEP
C
C PI = 4.*ATAN(1.)
C RAD = PI/180.
C THETA0 = INCID*RAD
C A = TAN(INCLIN)
C C2 = 1. + A*A
C
C DO 100 QI = -180, 180, STEP
C THETAD = QI
C THETAR = QI*RAD
C STH0 = SIN(THETA0)
C CTH0 = COS(THETA0)
C STH = SIN(THETAR)
C CTH = COS(THETAR)
C
C D = (STH0)**2. + A*CTH0*(2.*STH0 - A*CTH0)
C G = STH - STH0 + ALPHA*(CTH + CTH0)
C
C ECHOBI=C2/(2.*PI)*(2.*(1.-D/(2.*C2))*SIN(KOL*G)/G)**2
C WRITE(2, *) THETAD, ECHOBI
100 CONTINUE
```

STOP
END

G. PROGRAM SINUSMON

C THIS PROGRAM CALCULATES THE MONOSTATIC ECHO WIDTH OF A
C SINUSOIDAL SURFACE $z(x) = H \cdot \cos([2 \cdot \pi / d] \cdot x)$
C

C INPUT DATA:
C

C FREQ = FREQUENCY IN GHz
C

C H, d = PARAMETERS OF THE SINUSOIDAL SURFACE
C

C KOL = LIMIT OF INTEGRATION (KOL = K*L), WHERE :
C "K" IS THE PROPAGATION CONSTANT AND
C "L" IS THE ON THE X-AXIS SURFACE PROJECTION
C LENGTH
C

C STEP = ANGLE OF INCIDENCE INCREMENT
C

C M = NUMBER OF EQUIDISTANT POINTS BETWEEN THE TWO
C NORMALIZED LIMITS (0 AND 1) OF INTEGRATION
C (M ODD, M < 999).
C

C OUTPUT DATA:
C

C ECHOMO = NORMALIZED (WITH RESPECT TO THE WAVELENGTH)
C MONOSTATIC ECHO WIDTH, AS A FUNCTION OF THE
C INCIDENT ANGLE (THETA0) WHICH HERE (MONOSTATIC
C CASE) IS EQUAL TO: $2 \cdot \pi -$ OBSERVATION ANGLE.
C

C ECHO = NORMALIZED (WITH RESPECT TO THE SURFACE LENGTH
C $2 \cdot L$) MONOSTATIC ECHO WIDTH AS A FUNCTION OF THE
C ANGLE OF INCIDENCE, THETA0.
C

C REAL F(999)
C REAL K, KOL, KOLU, INCR, INCID, MAGN2_R
C COMPLEX J, R
C EXTERNAL FILON, FREAL, FIMAG
C COMMON K, H, W, THETA0, THETAR
C OPEN (UNIT=7, FILE='SINUSMON.DAT', FORM='FORMATTED',
& STATUS='UNKNOWN')
C READ(5,*) FREQ, H, d, KOL, STEP, M
C

C PI = 4.*ATAN(1.)
C W = 2.*PI/d
C RAD = PI/180.
C K = 20.*PI*FREQ/3.
C INCR = 1./M

```

C
DO 100 QI = 0., 90., STEP
  THETA0 = QI*PI
  THETAR = 2.*PI - THETA0
  TSO = KOL*(SIN(THETAR) - SIN(THETA0))
  SGN = SIGN(1,TSO)
  ABSTSO = ABS(TSO)

C
  I = 1
  DO 40 U = 0., 1., INCR
    KOLU = KOL*U
    F(I) = MOEVREAL(KOLU)
    I = I + 1
40 CONTINUE
  R1 = FILON(F,ABSTSO,0.,1.,M,999,1)

C
  I = 1
  DO 45 U = 0., 1., INCR
    KOLU = KOL*U
    F(I) = MOEVIMAG(KOLU)
    I = I + 1
45 CONTINUE
  R2 = FILON(F,ABSTSO,0.,1.,M,999,1)

C
  I = 1
  DO 50 U = 0., 1., INCR
    KOLU = KOL*U
    F(I) = MOODREAL(KOLU)
    I = I + 1
50 CONTINUE
  R3 = FILON(F,ABSTSO,0.,1.,M,999,2)

C
  I = 1
  DO 55 U = 0., 1., INCR
    KOLU = KOL*U
    F(I) = MOODIMAG(KOLU)
    I = I + 1
55 CONTINUE
  R4 = FILON(F,ABSTSO,0.,1.,M,999,2)
C
C      R : calculated value of the integral
C
  R = (R1 - SGN*R4) + J*(R2 + SGN*R3)
  RR = R1 - SGN*R4
  RI = R2 + SGN*R3
  MAGN2_R = RR*RR + RI*RI
C
  ECHO = MAGN2_R * KOL/8.
C
  ECHOMO = ECHO*KOL/PI
C
  WRITE(7,*) QI, ECHOMO, ECHO
100 CONTINUE

```

STOP
END

```
C *****
C REAL FUNCTION FILON (F, T, A, B, M, MAX, KEY)
C *****
C THIS PROGRAM COMPUTES  $\int_A^B [F(x) * \cos(Tx)] dx$  IF "KEY" = 1,
C AND  $\int_A^B [F(x) * \sin(Tx)] dx$  WHEN "KEY" = 2, USING FILON'S
C METHOD. FUNCTION "F(x)" IS ASSUMED TO BE GIVEN AS A
C TABLE OF FUNCTIONAL VALUES IN THE ARRAY AT "M"
C EQUIDISTANT POINTS FROM "A" TO "B", "M" ODD.
C "MAX" IS THE DIMENSION OF THE ARRAY DECLARED IN THE
C CALLING PROGRAM (FROM [REF. 9]).
C
C
C INTEGER KEY, M, N, I, MAX
C REAL F(MAX), AL, BE, GA, SUM, TH, H, S, C, S1, C1, S2, C2
C REAL F1, F2, SU, SU1, A1, A, B, T, TH2, TH4
C N = M - 1
C H = (B - A) / FLOAT (N)
C TH = T * H
C S = SIN (TH)
C C = COS (TH)
C TH2 = TH * TH
C IF (ABS (TH) .LE. 0.1) THEN
C   TH4 = TH2 * TH2
C   AL = 2. / 45. * TH * TH2 * (1.- TH2 / 7. + TH4 / 105.)
C   BE = 2. / 3. + 2. / 15. * TH2 - 4. / 105. * TH4
C   GA = 4. / 3. - 2. / 15. * TH2 + 1. / 210. * TH4
C ELSE
C   AL = 1. / TH + S * C / TH2 - 2. * S * S / (TH2 * TH)
C   BE = (2. + 2. * C * C - 4. * S * C / TH) / TH2
C   GA = 4. * (S / TH - C) / TH2
C END IF
C SUM = 0.0
C F1 = F (1)
C F2 = F (M)
C S1 = SIN (A * T)
C S2 = SIN (B * T)
C C1 = COS (A * T)
C C2 = COS (B * T)
C A1 = A + H
C GO TO (1, 2), KEY
1 SU = F2 * S2 - F1 * S1
  SU1 = -0.5 * (F2 * C2 - F1 * C1)
  DO 3 I = 2, N, 2
    SUM = SUM + F (I) * COS (A1 * T)
    A1 = A1 + H
    SU1 = SU1 + F (I+1) * COS (A1 * T)
```

```

3   A1 = A1 + H
   GO TO 4
2   IF (T .EQ. 0.) THEN
      FILON = 0.
      RETURN
   END IF
   SU = F1 * C1 - F2 * C2
   SU1 = -0.5 * (F2 * S2 - F1 * S1)
   DO 5 I = 2, N, 2
      SUM = SUM + F (I) * SIN (A1 * T)
      A1 = A1 + H
      SU1 = SU1 + F (I+1) * SIN (A1 * T)
5   A1 = A1 + H
4   FILON = H * (AL * SU + BE * SU1 + GA * SUM)
   RETURN
   END

C
C   *****
C   REAL FUNCTION MOEVREAL(RO)
C   *****
C
   REAL K
   COMPLEX J, BJC3, DJE, FE, EV, FACTOR
   COMMON K, H, W, THETA0, THETA

C
   STH0 = SIN(THETA0)
   CTH0 = COS(THETA0)
   STH = SIN(THETA)
   CTH = COS(THETA)
   WROK = W*RO/K
   SW = SIN(WROK)
   CW = COS(WROK)
   J = CMPLX(0.,1.)
   A = -H*W*SW
   B = -H*W*W/K*CW
   BA= ABS(B)
   C = SQRT(1.+ A*A)
   D = (STH0)*(STH0) - (A*CTH0)*(A*CTH0)
   E = B*CTH0/(C*C)
   C3 = C*C*C
   BJC3 = BA + J*C3
   DJE = D + J*E

C
   TSE = K*H*CW*(CTH - CTH0)
   FACTOR = 2.*C*CEXP(J*TSE)

C
   FE = BA/(2.*C3)*(1-BA/(4.*BJC3)) + C/(2.*BJC3)*DJE
   &      +J*(1+CTH0/C)
   EV = FACTOR*FE
   FEVREAL = REAL(EV)
   RETURN
   END

```

```

C      *****
C      REAL FUNCTION MOEVIMAG(RO)
C      *****
C
C      REAL K
C      COMPLEX J, BJC3, DJE, FE, EV, FACTOR
C      COMMON K, H, W, THETA0, THETA
C
C      STH0 = SIN(THETA0)
C      CTH0 = COS(THETA0)
C      STH  = SIN(THETA)
C      CTH  = COS(THETA)
C      WROK = W*RO/K
C      SW   = SIN(WROK)
C      CW   = COS(WROK)
C      J = CMPLX(0.,1.)
C      A = -H*W*SW
C      B = -H*W*W/K*CW
C      BA= ABS(B)
C      C = SQRT(1.+ A*A)
C      D = (STH0)*(STH0) - (A*CTH0)*(A*CTH0)
C      E = B*CTH0/(C*C)
C      C3 = C*C*C
C      BJC3 = BA + J*C3
C      DJE  = D + J*E
C
C      TSE = K*H*CW*(CTH - CTH0)
C      FACTOR = 2.*C*CEXP(J*TSE)
C
C      FE = BA/(2.*C3)*(1-BA/(4.*BJC3)) + C/(2.*BJC3)*DJE
&      +J*(1+CTH0/C)
C      EV = FACTOR*FE
C      FEVIMAG = AIMAG(EV)
C      RETURN
C      END
C
C      *****
C      REAL FUNCTION MOODREAL(RO)
C      *****
C
C      REAL K
C      COMPLEX J, BJC3, DJE, FO, OD, FACTOR
C      COMMON K, H, W, THETA0, THETA
C
C      STH0 = SIN(THETA0)
C      CTH0 = COS(THETA0)
C      STH  = SIN(THETA)
C      CTH  = COS(THETA)
C      WROK = W*RO/K
C      SW   = SIN(WROK)

```

```

CW = COS(WROK)
J = CMPLX(0.,1.)
A = -H*W*SW
B = -H*W*W/K*CW
BA= ABS(B)
C = SQRT(1.+ A*A)
D = 2.*A*STH0*CTH0
E = A*B*STH0/(C*C)
C3 = C*C*C
BJC3 = BA + J*C3
DJE = D + J*E
C
TSE = K*H*CW*(CTH - CTH0)
FACTOR = 2.*C*CEXP(J*TSE)
C
FO = C/(2.*BJC3)*DJE + J*A*STH0/C
OD = FACTOR*FO
FODREAL = REAL(OD)
RETURN
END
C
C
*****
REAL FUNCTION MOODIMAG(RO)
*****
C
C
REAL K
COMPLEX J, BJC3, DJE, FO, OD, FACTOR
COMMON K, H, W, THETA0, THETA
C
STH0 = SIN(THETA0)
CTH0 = COS(THETA0)
STH = SIN(THETA)
CTH = COS(THETA)
WROK = W*RO/K
SW = SIN(WROK)
CW = COS(WROK)
J = CMPLX(0.,1.)
A = -H*W*SW
B = -H*W*W/K*CW
BA= ABS(B)
C = SQRT(1.+ A*A)
D = 2.*A*STH0*CTH0
E = A*B*CTH0/(C*C)
C3 = C*C*C
BJC3 = BA + J*C3
DJE = D + J*E
C
TSE = K*H*CW*(CTH - CTH0)
FACTOR = 2.*C*CEXP(J*TSE)
C
FO = C/(2.*BJC3)*DJE + J*A*STH0/C
OD = FACTOR*FO

```

```
FODIMAG = AIMAG(OD)  
RETURN  
END
```



```

THETA0 = INCID*RAD
K = 20.*PI*FREQ/3.
INCR = 1./M
C
DO 100 QI = -90., 90., STEP
  THETAD = QI
  THETAR = THETAD*RAD
  TSO = KOL*(SIN(THETAR) - SIN(THETA0))
  SGN = SIGN(1,TSO)
  ABSTSO = ABS(TSO)
C
  I = 1
  DO 40 U = 0., 1., INCR
    KOLU = KOL*U
    F(I) = BIEVREAL(KOLU)
    I = I + 1
40  CONTINUE
  R1 = FILON(F,ABSTSO,0.,1.,M,999,1)
C
  I = 1
  DO 45 U = 0., 1., INCR
    KOLU = KOL*U
    F(I) = BIEVIMAG(KOLU)
    I = I + 1
45  CONTINUE
  R2 = FILON(F,ABSTSO,0.,1.,M,999,1)
C
  I = 1
  DO 50 U = 0., 1., INCR
    KOLU = KOL*U
    F(I) = BIODREAL(KOLU)
    I = I + 1
50  CONTINUE
  R3 = FILON(F,ABSTSO,0.,1.,M,999,2)
C
  I = 1
  DO 55 U = 0., 1., INCR
    KOLU = KOL*U
    F(I) = BIODIMAG(KOLU)
    I = I + 1
55  CONTINUE
  R4 = FILON(F,ABSTSO,0.,1.,M,999,2)
C
  R : calculated value of the integral
  R = (R1 - SGN*R4) + J*(R2 + SGN*R3)
  RR = R1 - SGN*R4
  RI = R2 + SGN*R3
  MAGN2_R = RR*RR + RI*RI
C
  ECHO = MAGN2_R * KOL/8.
C
  ECHOBI = ECHO/wavelength
C
  ECHOBI = ECHO*KOL/PI

```

```

        WRITE(8,*) QI, ECHOBI, ECHO
100    CONTINUE
        STOP
        END

C      *****
C      REAL FUNCTION BIEVREAL(RO)
C      *****
C
        REAL K
        COMPLEX J, BJC3, DJE, FE, EV, FACTOR
        COMMON K, H, W, THETA0, THETA

C
        STH0 = SIN(THETA0)
        CTH0 = COS(THETA0)
        STH  = SIN(THETA)
        CTH  = COS(THETA)
        WROK = W*RO/K
        SW   = SIN(WROK)
        CW   = COS(WROK)
        J    = CMPLX(0.,1.)
        A    = -H*W*SW
        B    = -H*W*W/K*CW
        BA   = ABS(B)
        C    = SQRT(1.+ A*A)
        D    = (STH0)*(STH0) - (A*CTH0)*(A*CTH0)
        E    = B*CTH0/(C*C)
        C3   = C*C*C
        BJC3 = BA + J*C3
        DJE  = D + J*E

C
        TSE = K*H*CW*(CTH - CTH0)

C
        FACTOR = 2.*C*CEXP(J*TSE)

C
        FE = BA/(2.*C3)*(1-BA/(4.*BJC3)) + C/(2.*BJC3)*DJE
&          +J*(1+CTH0/C)
        EV = FACTOR*FE

C
        FEVREAL = REAL(EV)
        RETURN
        END

C
C      *****
C      REAL FUNCTION BIEVIMAG(RO)
C      *****
C
        REAL K
        COMPLEX J, BJC3, DJE, FE, EV, FACTOR
        COMMON K, H, W, THETA0, THETA

C
        STH0 = SIN(THETA0)

```

```

CTH0 = COS (THETA0)
STH  = SIN (THETA)
CTH  = COS (THETA)
WROK = W*RO/K
SW   = SIN (WROK)
CW   = COS (WROK)
J = CMPLX (0., 1.)
A = -H*W*SW
B = -H*W*W/K*CW
BA= ABS (B)
C = SQRT (1.+ A*A)
D = (STH0)*(STH0) - (A*CTH0)*(A*CTH0)
E = B*CTH0/(C*C)
C3  = C*C*C
BJC3 = BA + J*C3
DJE  = D + J*E

C
TSE = K*H*CW*(CTH - CTH0)
FACTOR = 2.*C*CEXP(J*TSE)

C
FE = BA/(2.*C3)*(1-BA/(4.*BJC3)) + C/(2.*BJC3)*DJE
&      +J*(1+CTH0/C)
EV = FACTOR*FE
FEVIMAG = AIMAG (EV)
RETURN
END

C
C *****
C REAL FUNCTION BIODREAL(RO)
C *****
C
REAL K
COMPLEX J, BJC3, DJE, FO, OD, FACTOR
COMMON K, H, W, THETA0, THETA

C
STH0 = SIN (THETA0)
CTH0 = COS (THETA0)
STH  = SIN (THETA)
CTH  = COS (THETA)
WROK = W*RO/K
SW   = SIN (WROK)
CW   = COS (WROK)
J = CMPLX (0., 1.)
A = -H*W*SW
B = -H*W*W/K*CW
BA= ABS (B)
C = SQRT (1.+ A*A)
D = 2.*A*STH0*CTH0
E = -A*B*STH0/(C*C)
C3  = C*C*C
BJC3 = BA + J*C3
DJE  = D + J*E

```

```

C
TSE = K*H*CW*(CTH - CTH0)
FACTOR = 2.*C*CEXP(J*TSE)
C
FO = C/(2.*BJC3)*DJE + J*A*STH0/C
OD = FACTOR*FO
FODREAL = REAL(OD)
RETURN
END
C
*****
REAL FUNCTION BIODIMAG(RO)
*****
C
REAL K
COMPLEX J, BJC3, DJE, FO, OD, FACTOR
COMMON K, H, W, THETA0, THETA
C
STH0 = SIN(THETA0)
CTH0 = COS(THETA0)
STH = SIN(THETA)
CTH = COS(THETA)
WROK = W*RO/K
SW = SIN(WROK)
CW = COS(WROK)
J = CMPLX(0.,1.)
A = -H*W*SW
B = -H*W*W/K*CW
BA= ABS(B)
C = SQRT(1.+ A*A)
D = 2.*A*STH0*CTH0
E = A*B*STH0/(C*C)
C3 = C*C*C
BJC3 = BA + J*C3
DJE = D + J*E
C
TSE = K*H*CW*(CTH - CTH0)
FACTOR = 2.*C*CEXP(J*TSE)
C
FO = C/(2.*BJC3)*DJE + J*A*STH0/C
OD = FACTOR*FO
FODIMAG = AIMAG(OD)
RETURN
END

```

REFERENCES

1. Kriegsmann, G.A., Taflove, A. and Umashankar, K.R., "A New Formulation of Electromagnetic Wave Scattering Using an On-Surface Radiation Boundary Condition Approach," IEEE Trans. on Antennas and Propag., Vol. AP-35, No. 2, pp 153-161, February 1987.
2. Balanis, C.A., Advanced Engineering Electromagnetics, John Wiley & Sons, New York, 1989.
3. Berkey, D.D., Calculus, Saunders College Publishing, New York, 1988.
4. Balanis, C.A., Antenna Theory Analysis and Design, John Wiley & Sons, New York, 1982.
5. Zaki, K.A. and Neureuther, A.R., "Scattering from a Perfectly Conducting Surface with a Sinusoidal Height Profile: TE Polarization," IEEE Trans. on Antennas and Propag., Vol. AP-19, No. 2, pp 208-214, March 1971.
6. Tong, T. C-H and Senior, T.B.A., "Scattering of Electromagnetic Waves by a Periodic Surface with Arbitrary Profile," The University of Michigan Scientific Report, No. 13, pp. 28-42, April 1972.
7. Millar, R.F., "On the Rayleigh Assumption in Scattering by a Periodic Surface. II," Proc. Camp. Phil. Soc., Vol. 69, No. 21, pp. 217-225, 1971.
8. Ruck, G.T., Barrick, D.E., Stuart, W.D., and Krichbaum, C.K., Radar Cross Section Handbook, Vol 2, Plenum Press, New York, 1970.
9. Davis, P.J. and Rabinowitz, P., Methods of Numerical Integration, Academic Press, New York, 1984.

INITIAL DISTRIBUTION LIST

Defense Technical Information Center Cameron Station Alexandria, VA 22304-6145	2
Library, Code 52 Naval Postgraduate School Monterey, CA 93943-5100	2
Chairman, Code EC Department of Electrical and Computer Engineering Naval Postgraduate School Monterey, CA 93943-5000	1
Prof. R. Jaraswamy, Code EC/Js Naval Postgraduate School Monterey, CA 93943-5000	1
Prof. R. C. Robertson, Code EC/Rc Naval Postgraduate School Monterey, CA 93943-5000	1
LTJG Spyridon Konidaris Spartis 126 Kalithea 176 75 Athens Greece	2
Embassy of Greece Naval Attache 2228 Massachusetts Ave., N.W. Washington, DC 20008	4
Dr. Peter Zavitsanos P.O. BOX 412 Gwynedd Valley, PA 19437	1
Anastasios Konidaris 8900 Ridge Ave. Philadelphia, PA 19128	1